kappaB activation by vaccinia protein N1 occur via distinct binding surfaces and make different contributions to virulence. PLoS Pathog. 7:e1002430. doi:10.1371/journal.ppat.1002430.
46. **O'Connor L, et al.** 1998. Bim: a novel member of the Bcl-2 family that promotes apoptosis. EMBO J. 17:384–395.
47. **Oltersdorf T, et al.** 2005. An inhibitor of Bcl-2 family proteins induces regression of solid tumours. Nature 435:677–681.
48. **Postigo A, Cross JR, Downward J, Way M.** 2006. Interaction of F1L with the BH3 domain of Bak is responsible for inhibiting vaccinia-induced apoptosis. Cell Death Differ. 13:1651–1662.
49. **Postigo A, Martin MC, Dodding MP, Way M.** 2009. Vaccinia-induced epidermal growth factor receptor-MEK signalling and the anti-apoptotic protein F1L synergize to suppress cell death during infection. Cell Microbiol. 11:1208–1218.
50. **Postigo A, Way M.** 2012. The vaccinia virus-encoded Bcl-2 homologues do not act as direct Bax inhibitors. J. Virol. 86:203–213.
51. **Roulston A, Marcellus RC, Branton PE.** 1999. Viruses and apoptosis. Annu. Rev. Microbiol. 53:577–628.
52. **Sarid R, Sato T, Bohenzky RA, Russo JJ, Chang Y.** 1997. Kaposi's sarcoma-associated herpesvirus encodes a functional Bcl-2 homologue. Nat. Med. 3:293–298.
53. **Schneider P, et al.** 1998. Conversion of membrane-bound Fas(CD95) ligand to its soluble form is associated with downregulation of its proapoptotic activity and loss of liver toxicity. J. Exp. Med. 187:1205–1213.
54. **Smith CA.** 1995. A novel viral homologue of Bcl-2 and Ced-9. Trends Cell Biol. 5:344.
55. **Strasser A.** 2005. The role of BH3-only proteins in the immune system. Nat. Rev. Immunol. 5:189–200.
56. **Taylor JM, Quilty D, Banadyga L, Barry M.** 2006. The vaccinia virus protein F1L interacts with Bim and inhibits activation of the proapoptotic protein Bax. J. Biol. Chem. 281:39728–39739.
57. **Thompson JD, Higgins DG, Gibson TJ.** 1994. CLUSTAL W: improving the sensitivity of progressive multiple sequence alignment through sequence weighting, position-specific gap penalties and weight matrix choice. Nucleic Acids Res. 22:4673–4680.
58. **van Delft MF, et al.** 2006. The BH3 mimetic ABT-737 targets selective Bcl-2 proteins and efficiently induces apoptosis via Bak/Bax if Mcl-1 is neutralized. Cancer Cell 10:389–399.
59. **Wang G, et al.** 2004. Myxoma virus M11L prevents apoptosis through constitutive interaction with Bak. J. Virol. 78:7097–7111.
60. **Wang GQ, et al.** 2001. Resistance to granzyme B-mediated cytochrome *c* release in Bak-deficient cells. J. Exp. Med. 194:1325–1337.
61. **Wasilenko ST, Banadyga L, Bond D, Barry M.** 2005. The vaccinia virus F1L protein interacts with the proapoptotic protein Bak and inhibits Bak activation. J. Virol. 79:14031–14043.
62. **Wasilenko ST, Meyers AF, Vander Helm K, Barry M.** 2001. Vaccinia virus infection disarms the mitochondrion-mediated pathway of the apoptotic cascade by modulating the permeability transition pore. J. Virol. 75:11437–11448.
63. **Wasilenko ST, Stewart TL, Meyers AF, Barry M.** 2003. Vaccinia virus encodes a previously uncharacterized mitochondrial-associated inhibitor of apoptosis. Proc. Natl. Acad. Sci. U. S. A. 100:14345–14350.
64. **Westphal D, et al.** 2007. A novel Bcl-2-like inhibitor of apoptosis is encoded by the parapoxvirus ORF virus. J. Virol. 81:7178–7188.
65. **Westphal D, et al.** 2009. The orf virus inhibitor of apoptosis functions in a Bcl-2-like manner, binding and neutralizing a set of BH3-only proteins and active Bax. Apoptosis 14:1317–1330.
66. **White E, et al.** 1992. The 19-kilodalton adenovirus E1B transforming protein inhibits programmed cell death and prevents cytolysis by tumor necrosis factor α. Mol. Cell. Biol. 12:2570–2580.
67. **Willis SN, et al.** 2005. Pro-apoptotic Bak is sequestered by Mcl-1 and Bcl-xL, but not Bcl-2, until displaced by BH3-only proteins. Genes Dev. 19:1294–1305.
68. **Youle RJ, Strasser A.** 2008. The BCL-2 protein family: opposing activities that mediate cell death. Nat. Rev. Mol. Cell Biol. 9:47–59.

Cell PRESS

Immunity
Article

A Cluster of Interferon-γ-Inducible p65 GTPases Plays a Critical Role in Host Defense against *Toxoplasma gondii*

Masahiro Yamamoto,[1,2,3,4,7,10,*] Megumi Okuyama,[1,10] Ji Su Ma,[1,2,3,4] Taishi Kimura,[1,2] Naganori Kamiyama,[1,2,3,4] Hiroyuki Saiga,[1] Jun Ohshima,[1,2,3,4] Miwa Sasai,[4] Hisako Kayama,[1,2,7] Toru Okamoto,[5,8] David C.S. Huang,[8] Dominique Soldati-Favre,[9] Kyoji Horie,[6] Junji Takeda,[6] and Kiyoshi Takeda[1,2,7,*]

[1]Department of Microbiology and Immunology, Graduate School of Medicine
[2]Laboratory of Mucosal Immunology, WPI Immunology Frontier Research Center
[3]Laboratory of Immunoparasitology, WPI Immunology Frontier Research Center
[4]Department of Immunoparasitology, Research Institute for Microbial Diseases
[5]Department of Molecular Virology, Research Institute for Microbial Diseases
[6]Department of Social and Environmental Medicine, Graduate School of Medicine
Osaka University, Yamadaoka, Suita, Osaka 565-0871, Japan
[7]Core Research for Evolutional Science and Technology, Japan Science and Technology Agency, Saitama 332-0012, Japan
[8]The Walter and Eliza Hall Institute of Medical Research and Department of Medical Biology, University of Melbourne, Parkville, VIC 3052, Australia
[9]Department of Microbiology and Molecular Medicine, CMU, University of Geneva, 1211 Geneva 4, Switzerland
[10]These authors contributed equally to this work
*Correspondence: myamamoto@biken.osaka-u.ac.jp (M.Y.), ktakeda@ongene.med.osaka-u.ac.jp (K.T.)
http://dx.doi.org/10.1016/j.immuni.2012.06.009

SUMMARY

Interferon-γ (IFN-γ) is essential for host defense against intracellular pathogens. Stimulation of innate immune cells by IFN-γ upregulates ~2,000 effector genes such as immunity-related GTPases including p65 guanylate-binding protein (Gbp) family genes. We show that a cluster of *Gbp* genes was required for host cellular immunity against the intracellular parasite *Toxoplasma gondii*. We generated mice deficient for all six *Gbp* genes located on chromosome 3 (Gbp^{chr3}) by targeted chromosome engineering. Mice lacking Gbp^{chr3} were highly susceptible to *T. gondii* infection, resulting in increased parasite burden in immune organs. Furthermore, Gbp^{chr3}-deleted macrophages were defective in IFN-γ-mediated suppression of *T. gondii* intracellular growth and recruitment of IFN-γ-inducible p47 GTPase Irgb6 to the parasitophorous vacuole. In addition, some members of Gbp^{chr3} restored the protective response against *T. gondii* in Gbp^{chr3}-deleted cells. Our results suggest that Gbp^{chr3} play a pivotal role in anti-*T. gondii* host defense by controlling IFN-γ-mediated Irgb6-dependent cellular innate immunity.

INTRODUCTION

Interferon-γ (IFN-γ) is an important T helper 1 (Th1) cell cytokine that strongly suppresses the growth and survival of intracellular pathogens (Boehm et al., 1997). Stimulation of innate immune cells such as macrophages and dendritic cells by IFN-γ results in robust gene expression of a number of effector molecules. These include immunity-related GTPases such as the Mx proteins, immunity-related p47 GTPases (Irgs), and p65 guanylate-binding proteins (Gbps) (Shenoy et al., 2007; Taylor et al., 2004). Mx proteins have been shown to participate in host defense against RNA viruses such as influenza and vesicular stomatitis virus (Sadler and Williams, 2008). Among the Irgs, mice deficient in Irgm1 (Lrg-47) are highly susceptible to *Listeria*, *Salmonella*, and mycobacteria (Deretic, 2006; MacMicking, 2004). Furthermore, Gbps have recently been shown to induce antibacterial responses involving phagocytic oxidases, autophagic effectors, and inflammasome (Kim et al., 2011; Shenoy et al., 2012). Thus, IFN-γ-inducible immunity-related GTPases play pivotal roles in antiviral and antibacterial immune systems.

Toxoplasma gondii is an obligatory intracellular protozoan parasite that infects virtually all warm-blooded vertebrates including human and mouse (Boothroyd, 2009; Israelski and Remington, 1993). Infection of immunocompromised individuals such as those suffering from AIDS or those being treated with chemotherapy often leads to fatal toxoplasmosis encephalitis (Montoya and Remington, 2008). Innate immune cells, which recognize microbial components mainly via Toll-like receptors (TLRs) and the chemokine receptor CCR5, are essential in controlling *T. gondii* infection via the production of proinflammatory cytokines such as interleukin-12 (IL-12) (Aliberti et al., 2003; Hunter and Remington, 1995; Yarovinsky and Sher, 2006). IL-12 potentiates polarization of naive T cells to Th1 cells, from which IFN-γ is produced in an antigen-dependent fashion (Trinchieri, 2003; Whitmarsh et al., 2011). IFN-γ-inducible GTPases are also important for the inhibition of *T. gondii* growth by IFN-γ. Mice lacking Irgm1, Irgd (Irg-47), Irgm3 (Igtp), or Irga6 (Iigp1) are susceptible to acute and chronic infection (Collazo et al., 2001; Howard et al., 2011; Taylor et al., 2000). IRGs are recruited to the parasitophorous vacuole (PV), a membrane formed during invasion that is maintained to surround the intracellular

replicating parasites. Accumulation of Irgs eventually leads to disruption of the integrity of the PV membranes (Howard et al., 2011; Ling et al., 2006; Taylor et al., 2007; Zhao et al., 2008).

Not only Irgs but also Gbps are known to accumulate around the PV shortly after *T. gondii* invasion (Degrandi et al., 2007). Moreover, because virulent strains of *T. gondii* inhibit the recruitment of Gbps around the PV (Degrandi et al., 2007; Virreira Winter et al., 2011), Gbps are considered anti-*T. gondii* defensive factors. Among Gbps, Gbp1 and Gbp2 are reported to modulate cellular proliferation (Gorbacheva et al., 2002; Guenzi et al., 2001). In addition, Gbp1 is involved in the regulation of matrix metalloproteinase 1 in cancer cell lines (Guenzi et al., 2003; Li et al., 2011). Although in vitro studies have been reported, the physiological protective role of Gbps against *T. gondii* remains uncertain. The mouse genome carries 13 *Gbp* genes (11 active members and 2 pseudogenes) that are organized in clusters and share a high degree of homology (Kresse et al., 2008). Six and seven family members are tandemly aligned on chromosomes 3 and 5, respectively (Kresse et al., 2008). Such a complex configuration has hampered in vivo investigation of the *Gbp* genes through genetic approaches.

To elucidate the in vivo functional contribution of the Gbps to host defense against *T. gondii*, we have generated mice lacking the entire cluster of *Gbp*s on chromosome 3 (Gbp^{chr3}) by Cre-loxP-based chromosome engineering. Gbp^{chr3}-deleted mice were highly susceptible to *T. gondii* infection with a considerably increased parasite burden in tissues. Furthermore, Gbp^{chr3}-deleted macrophages showed defective suppression of parasite growth in response to IFN-γ. Although parasite infection-induced production of oxidants and proinflammatory cytokines as well as autophagy-related 4b (Atg4b) recruitment to the parasites were normal, IFN-γ-induced disruption of the PV membrane and localization of Irgs such as Irgb6 and Irgb10 to the PV were compromised in Gbp^{chr3}-deleted cells. Moreover, endogenous Gbps colocalized and interacted with Irgb6. The reintroduction of *Gbp1*, *Gbp5*, or *Gbp7* into Gbp^{chr3}-deleted cells *partially* restored the IFN-γ-dependent anti-*T. gondii* response. Taken together, these results demonstrate that this cluster of Gbps has a defensive function against *T. gondii* by positively regulating IFN-γ-inducible Irgb6-dependent cellular innate immunity.

RESULTS

Generation of Mice Lacking the Entire *Gbp* Locus on Chromosome 3

To assess the anti-*T. gondii* immunity of Gbp^{chr3} in vivo, we generated embryonic stem (ES) cells possessing loxP sites at the most proximal and distal loci from the centromere in the gene cluster (*Gbp5* and *Gbp2ps*, respectively) by sequential conventional gene targeting methods (Figure 1A and Figure S1 available online). Deletion of the entire Gbp^{chr3} locus spanning 173 kb was achieved by crossing the F1 mice with CAG-Cre transgenic mice and was confirmed by Southern blotting and PCR (Figures 1B and 1C). Gbp^{chr3}-deleted mice were successfully obtained by intercrossing heterozygous mice, were born at the expected Mendelian ratio, and were healthy and normal in specific-pathogen-free conditions (Figure 1D). Under nonstimulated conditions, Gbp^{chr3}-deleted mice showed normal parameters of cellular immunity (Figure S1H). To test whether the expression of Gbp^{chr3} was correctly ablated in Gbp^{chr3}-deleted cells, we confirmed by quantitative RT-PCR that the mRNAs derived from Gbp^{chr3} (*Gbp1*, *Gbp2*, *Gbp3*, *Gbp5*, *Gbp7*, and *Gbp2ps*) were not induced in response to IFN-γ in Gbp^{chr3}-deleted cells (Figure 1E). On the other hand, mRNAs for the Gbps on chromosome 5 (*Gbp4*, *Gbp6*, *Gbp8*, *Gbp9*, *Gbp10*, and *Gbp11*) were normally induced. We further analyzed Gbp^{chr3} expression by protein immunoblotting and found that Gbp1, Gbp2, and Gbp5 proteins were not detected. A weak signal was observed when we performed blotting with Gbp1-5 monoclonal antibodies that are raised against amino acids 1–300 mapping at the N terminus of human GBP1 and that recognize a shared epitope among Gbp1, Gbp2, Gbp3, Gbp4, and Gbp5. Expression of the gene encoding Gbp4, which is not disrupted in Gbp^{chr3}-deleted cells, could account for this weak signal (Figure 1F).

Gbp^{chr3} Confer Resistance to *T. gondii* In Vivo

First, mice lacking *Gbp2ps* alone or deficient in both *Gbp2ps* and *Gbp5* were infected intraperitoneally with the avirulent *T. gondii* strain ME49 and shown to exhibit survival rates similar to those of wild-type mice (Figures S1C and S1F). In contrast, infection of Gbp^{chr3}-deleted mice revealed that these mutant mice were highly prone to die after *T. gondii* infection (Figure 2A). Because Gbp1 and Gbp5 were recently shown to be involved in host defense against *Listeria monocytogenes* (Kim et al., 2011; Shenoy et al., 2007), we challenged Gbp^{chr3}-deleted mice with *L. monocytogenes* by intraperitoneal injection. Wild-type and Gbp^{chr3}-deleted mice exhibited comparable bacterial burdens in tissues and survival rate (Figures S2A and S2B). To monitor the course of infection more accurately, we generated transgenic ME49 *T. gondii* expressing luciferase and monitored the kinetics by in vivo imaging in wild-type and Gbp^{chr3}-deleted mice infected with 10^2 parasites. Significant increases in parasite number were observed at days 7, 8, and 9 in Gbp^{chr3}-deleted mice compared with those in wild-type mice (Figures 2B and S2C). We next compared parasite burdens in organs from the infected mice. The parasite load showed an excellent correlation with luciferase counts in vitro (Figures S2D and S2E). We collected the spleens and mesenteric lymph nodes from wild-type or Gbp^{chr3}-deleted mice 9 days after a challenge with luciferase-expressing parasites and calculated the parasite numbers according to the luciferase signal. The parasite load in the tissues originating from Gbp^{chr3}-deleted mice was markedly elevated in comparison with that from wild-type mice (Figure 2C). Taken together, these findings demonstrate that Gbp^{chr3} protects against the spreading and proliferation of *T. gondii* in vivo.

Next we examined immune responses during parasite infection in wild-type and Gbp^{chr3}-deleted mice. IL-12 is important for the development of type I immunity, in which IFN-γ-producing $CD4^+$ and $CD8^+$ T cells play central roles for anti-*T. gondii* responses (Hunter et al., 1995). The concentrations of IL-12p40 and IFN-γ measured in sera were similarly increased in wild-type and Gbp^{chr3}-deleted mice infected with *T. gondii* (Figure 2D). Furthermore, cellularity in spleens and IFN-γ production from splenic $CD4^+$ and $CD8^+$ T cells in response to anti-CD3 was comparable in wild-type and Gbp^{chr3}-deleted mice (Figures 2E and S2F), suggesting that the high susceptibility to *T. gondii* in Gbp^{chr3}-deleted mice was not due to defects in production of IL-12 or IFN-γ or in T cell responses.

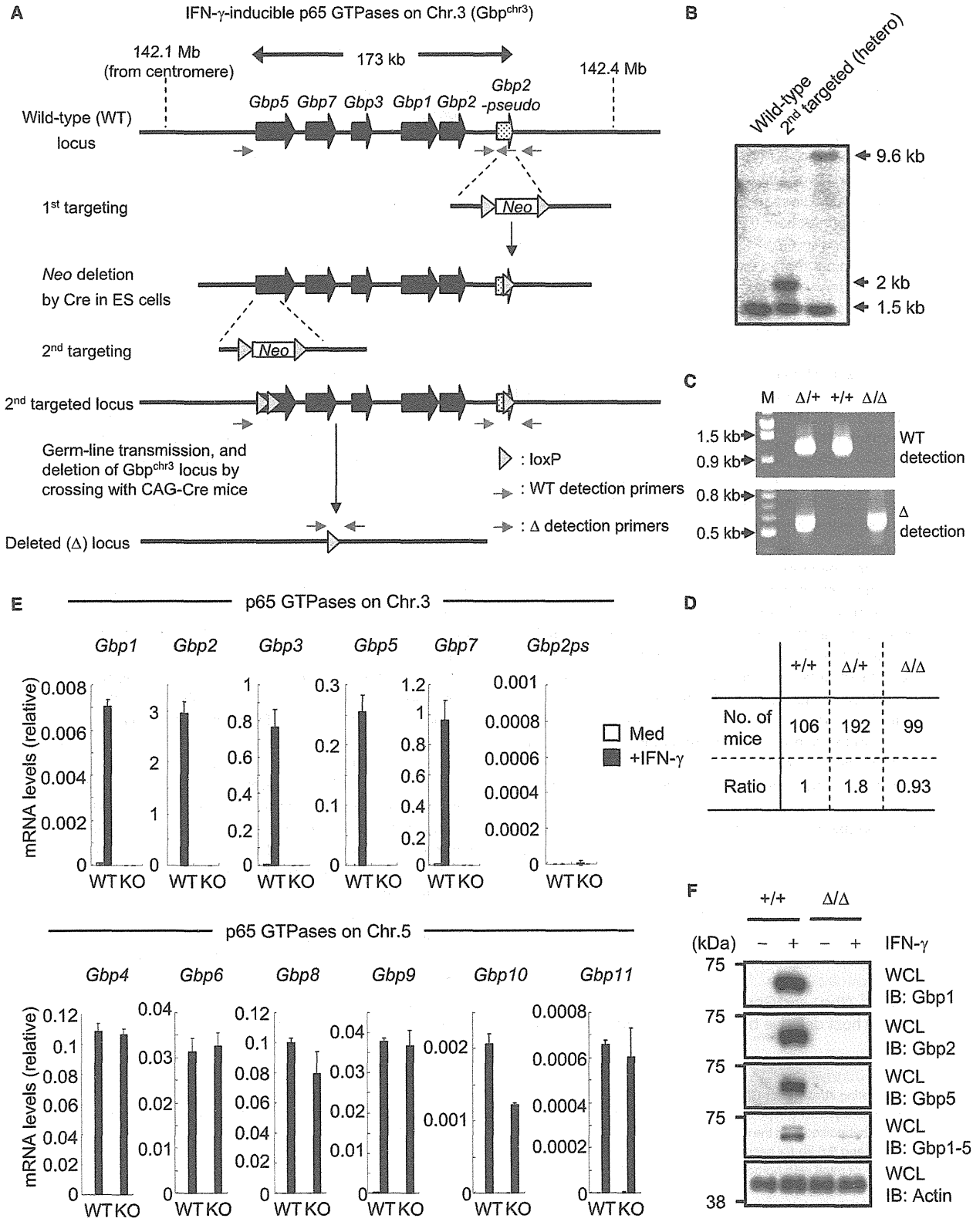

	+/+	Δ/+	Δ/Δ
No. of mice	106	192	99
Ratio	1	1.8	0.93

Gbp^{chr3} Are Essential for IFN-γ-Induced Reduction of *T. gondii* Infection in Macrophages

Macrophages play a vital role in IFN-γ-mediated cellular innate immunity against *T. gondii* (Suzuki et al., 1988). Peritoneal macrophages represent a major cell type targeted by the parasite at the early stage after intraperitoneal infection (Jensen et al., 2011). To analyze the impact of Gbp^{chr3} deficiency in this cell type, we infected wild-type or Gbp^{chr3}-deleted peritoneal macrophages with *T. gondii* expressing luciferase in the presence of IFN-γ and assessed the luciferase units at 1, 12, 24, 36, or 48 hr postinfection (Figure 3A). We observed higher luciferase emissions in Gbp^{chr3}-deleted cells than in wild-type cells at all time points tested except for 1 hr. Next, we analyzed the IFN-γ-dependent reduction of parasite burden by counting parasite numbers and the luciferase units in macrophages and mouse embryonic fibroblasts (MEFs) from wild-type or Gbp^{chr3}-deleted mice. The dose-dependent reduction of parasite numbers and luciferase signals in both cell types lacking Gbp^{chr3} was less pronounced than that in wild-type cells (Figures 3B and S3A). On the other hand, costimulation of tumor necrosis factor-α (TNF-α), which is known to strongly enhance antitoxoplasmal activity in macrophage in combination with IFN-γ (Sibley et al., 1991), abrogated the difference between wild-type and Gbp^{chr3}-deleted cells (Figure S3B). These data suggested a selective impairment in IFN-γ-mediated reduction of parasite burden.

IFN-γ leads to inhibition of *T. gondii* proliferation and promotes its clearance from macrophages (Ling et al., 2006). To measure clearance, we next used confocal microscopy to compare the degree of parasite infection and growth in macrophages isolated from wild-type or Gbp^{chr3}-deleted mice. At 5 hr postinfection, the percentage of cells infected with the parasites was comparable between wild-type and Gbp^{chr3}-deleted mice (Figure 3C). In contrast, the infection rate of IFN-γ-stimulated macrophages from Gbp^{chr3}-deleted mice was remarkably higher than that from wild-type cells after 20 hr (Figures 3C, 3D, and S3C). Next, we compared the rate of parasite replication in wild-type and Gbp^{chr3}-deleted macrophages in the presence of IFN-γ by counting the parasite numbers per PV. In Gbp^{chr3}-deleted cells, the number of parasites per PV was modestly increased compared with that in wild-type cells (Figures 3D and 3E), indicating that Gbp^{chr3} are not only required for clearance but also inhibit parasite replication in IFN-γ-stimulated macrophages.

Impact of Gbp^{chr3} Deficiency on IFN-γ-Mediated Anti-*T. gondii* Response

Among Gbp^{chr3}, Gbp1 and Gbp7 have been shown to participate in antibacterial host defense by inducing an oxidative response and recruiting autophagy effectors such as Atg4b to *L. monocytogenes* and *Mycobacterium bovis* (Kim et al., 2011). To test whether these mechanisms also apply to anti-*T. gondii* defense, we first measured IFN-γ-induced oxide ion (O^{2-}) production in wild-type or Gbp^{chr3}-deleted cells infected with *T. gondii* (Figure 4A). The O^{2-} production in Gbp^{chr3}-deleted macrophages was normally enhanced. Next, we examined Atg4b recruitment to the parasite by confocal microscopy. As observed for pathogenic bacteria, Atg4b colocalized with intracellular *T. gondii* in wild-type cells. The increased recruitment of Atg4b to parasites in Gbp^{chr3}-deleted macrophages was not altered during the course of infection (Figures 4B and S4A). Taken together, these results suggest that the anti-*T. gondii* action of Gbp^{chr3} operates independently of O^{2-} and Atg4b recruitment.

IFN-γ is also known to augment proinflammatory cytokine production in response to TLR ligands, and *T. gondii* possesses a profilin that can serve as a TLR11 ligand called profilin-like molecule (Plattner et al., 2008; Yarovinsky et al., 2005). We analyzed the production of proinflammatory cytokines in macrophages. Production of tumor necrosis factor α, IL-6, and IL-12p40 in IFN-γ-treated Gbp^{chr3}-deleted cells in response to *T. gondii* infection or lipopolysaccharide (LPS) was normal (Figure S4B), indicating that Gbp^{chr3} are dispensable for IFN-γ-mediated production of proinflammatory cytokines.

Because nitric oxide (NO) was previously reported to inhibit *T. gondii* replication in vitro (Adams et al., 1990), we assessed NO production in wild-type and Gbp^{chr3}-deleted cells. Nonstimulated, *T. gondii*-infected, or LPS-treated macrophages from Gbp^{chr3}-deleted mice produced similar concentrations of nitrite ion (NO^{2-}) compared with that produced by wild-type cells (Figure S4C). Furthermore, hepatic expression of iNOS mRNAs was unchanged between wild-type and Gbp^{chr3}-deleted mice in *T. gondii* infection (Figure S4D). In spite of normal NO production in Gbp^{chr3}-deleted macrophages (Figure S4C), the inhibition of the parasite replication was modestly impaired by the Gbp^{chr3} deficiency (Figure 3E). To examine whether NO is involved in inhibition of parasite replication in Gbp^{chr3}-deleted cells, we compared the replication in Gbp^{chr3}-deleted cells between those untreated and those treated with aminoguanidine (AG), an NO inhibitor (Figure 4C). Although the infection rate was not affected at all, AG-treated Gbp^{chr3}-deleted cells contained significantly larger numbers of the parasites per vacuole than control cells, indicating that NO indeed plays a major role in inhibition of *T. gondii* replication in Gbp^{chr3}-deleted macrophages in vitro. To further determine relative importance of Gbp^{chr3} in the IFN-γ-dependent anti-*T. gondii* response in vivo, we compared parasite burdens and the survival rate of wild-type and

Figure 1. Generation of Gbp^{chr3}-Deleted Mice

(A) The gene targeting strategy for Gbp^{chr3} locus by chromosome engineering.

(B) Southern blot analysis of offspring from the heterozygote intercrosses. Genomic DNA was extracted from mouse tails, digested with KpnI and PstI, electrophoresed, and hybridized with the radiolabelled probe indicated in Figure S1G. Southern blotting resulted in a 1.5 kb band for wild-type locus, a 2.0 kb band for deleted (Δ) locus, and 9.6 kb for second targeted locus.

(C) PCR detection of mice with homozygous deletion of Gbp^{chr3} locus. Primers used are denoted in (A).

(D) Numbers of offspring by intercross of heterozygous (Δ/+) mice.

(E) Quantitative PCR analysis of the expression of the indicated Gbp mRNA in wild-type (WT) or Gbp^{chr3}-deleted (KO) peritoneal macrophages unstimulated or stimulated with 100 ng/ml IFN-γ.

(F) Peritoneal macrophages treated with 100 ng/ml IFN-γ for 24 hr were lysed. The lysates were detected by protein immunoblot with the indicated Abs.

Data are representative of two (B, C, E) and three (F) independent experiments. See also Figure S1.

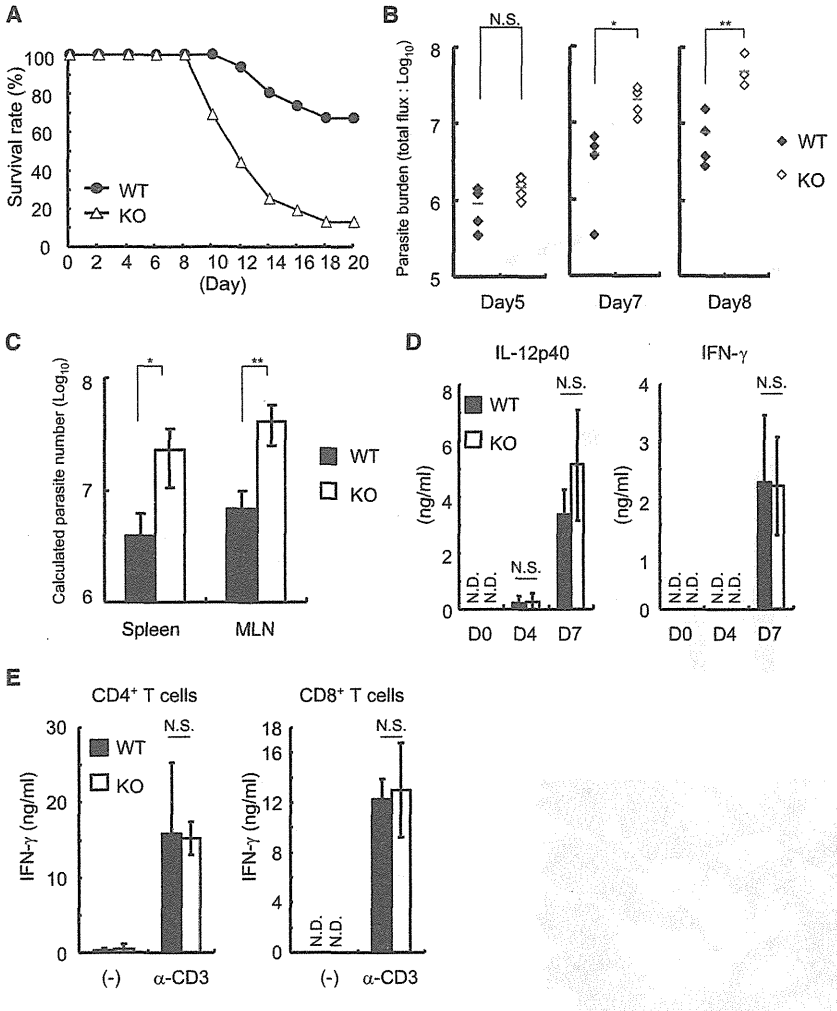

Figure 2. *Gbp*^{chr3}-Deleted Mice Are Highly Susceptible to *T. gondii*

(A) Wild-type (n = 15) or *Gbp*^{chr3}-deleted (KO) (n = 16) mice were infected with 1 × 10^2 *T. gondii*, and the survival rates were monitored for 20 days.

(B) Total photon emission analysis from wild-type or *Gbp*^{chr3}-deleted mice (n = 4 per group) infected with 1 × 10^2 ME49 *T. gondii* luciferase-expressing parasites at days 5, 7, or 8 after infection. The flux (photons/s/cm^2/sr) was determined as a measure of parasite burden. *p < 0.01, **p < 0.02.

(C) Quantification of parasites in indicated tissues from 4 mice per group at day 9 postinfection by the standard curve in Figure S2. Indicated values are means ± SD of quadruplicates. *p < 0.005, **p < 0.03.

(D) Sera were taken from indicated mice (n = 4 per group) at the indicated time postinfection of 1 × 10^2 *T. gondii*. Serum concentrations of the indicated cytokines were determined by ELISA.

(E) Splenic CD4$^+$ or CD8$^+$ T cells from indicated mice (n = 4 per group) at day 7 postinfection of 1 × 10^2 *T. gondii* were cultured in the presence of 5 μg/ml plate-bound anti-CD3 for 24 hr. Concentration of IFN-γ in the culture supernatants was measured by ELISA. Indicated values are means ± SD of triplicates.

N.D., not detected; N.S., not significant. Data are representative of three (C) and two (B, D, E) independent experiments. Data in (A) are pooled from three independent experiments with five or six mice per group. See also Figure S2.

Gbp^{chr3}-deleted mice treated with anti-IFN-γ (Figures 4D and 4E). Although the mortality was not increased by anti-IFN-γ treatment in *Gbp*^{chr3}-deleted mice (Figure 4D), *Gbp*^{chr3}-deleted mice treated with anti-IFN-γ displayed much higher parasite burdens than did control IgG-treated groups (Figure 4E). These results indicated that Gbp^{chr3} do not fully account for the IFN-γ-dependent anti-*T. gondii* immunity in vitro and in vivo.

Impaired Disruption of the PV Membrane in *Gbp*^{chr3}-Deleted Macrophages

Gbp^{chr3} deficiency resulted in compromised IFN-γ-induced clearance of *T. gondii* in macrophages (Figure 3). The killing by IFN-γ-activated macrophages is accompanied by blebbing of the PV membrane shortly after parasite entry (Ling et al., 2006; Zhao et al., 2008). Therefore, we examined by electron microcopy the morphology of the parasite PV membrane in wild-type and *Gbp*^{chr3}-deleted macrophages 6 hr postinfection. Blebbing and vesiculation were easily detectable in the vicinity of the parasite PV membrane in wild-type cells (Figure 5A). In sharp contrast, in *Gbp*^{chr3}-deleted cells the parasites were surrounded by a continuous intact PV membrane (Figure 5B), suggesting that Gbps affect IFN-γ-induced clearance of *T. gondii* shortly after invasion. Moreover, 24 hr postinfection, a markedly increased number of dead parasites with damaged parasite membranes or no PV membranes were observed in wild-type cells compared with those in *Gbp*^{chr3}-deleted cells (Figure 5C and data not shown).

Defective Irgb6 Recruitment to PVs in *Gbp*^{chr3}-Deleted Macrophages

A previous study demonstrated that macrophages lacking the autophagy protein Atg5 exhibit defective blebbing of the *T. gondii* PV (Zhao et al., 2008), which is reminiscent of the phenotype observed in *Gbp*^{chr3}-deleted cells (Figure 5B). Atg5 has been reported to be required for the recruitment of Irga6 to the PV (Zhao et al., 2008). Irgs including Irga6 (also known as IIGP1), Irgb6 (TGTP), and Irgb10 were shown to be phosphorylated and dampened by *T. gondii* ROP18, a parasite-secreted kinase that acts as a virulence effector molecule (Fentress et al., 2010; Steinfeldt et al., 2010). The CTG strain of *T. gondii* produces an extremely low *ROP18* mRNA expression (Boothroyd and Dubremetz, 2008; Saeij et al., 2006; Taylor et al., 2006); hence the CTG parasites as well as ME49 are permissive for Irg recruitment to the PV membrane (Saeij et al., 2006; Taylor et al., 2006). By using the CTG strain expressing luciferase, we found that the IFN-γ-dependent decrease in CTG parasites was impaired in *Gbp*^{chr3}-deleted macrophages (Figure 6A),

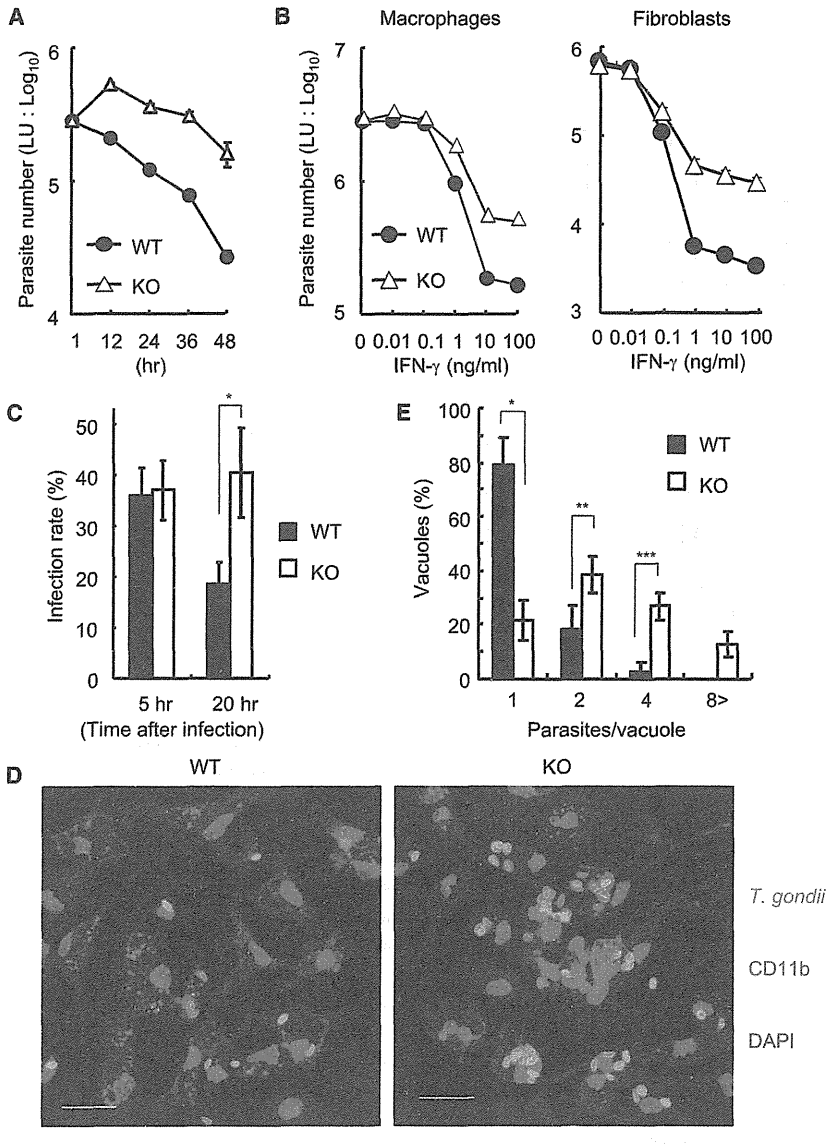

Figure 3. Impaired IFN-γ-Mediated Parasite Clearance in *Gbp*^{chr3}-Deleted Macrophages

(A) Wild-type (WT) and *Gbp*^{chr3}-deleted (KO) peritoneal macrophages were treated with 100 ng/ml IFN-γ for 24 hr. IFN-γ-treated cells were infected with ME49 *T. gondii* expressing lucifease (moi = 0.5) and harvested at the indicated point postinfection. The luciferase units (LU) were assayed with the lysates. Indicated values are means ± SD of triplicates.

(B) WT and KO peritoneal macrophages or MEFs were untreated or treated with the indicated concentrations of IFN-γ for 24 hr. Untreated or IFN-γ-treated cells were infected with ME49 *T. gondii* expressing luciferase (moi = 0.5) and harvested at 36 hr postinfection. The LU were assayed with the lysates. Indicated values are means ± SD of triplicates.

(C) The percentage of WT and KO macrophages containing at least one *T. gondii* parasite at the indicated points postinfection. Indicated values are means ± SD of triplicates. $^{**}p < 0.03$.

(D) WT and KO peritoneal macrophages were treated with 100 ng/ml IFN-γ for 24 hr. IFN-γ-treated cells were infected with ME49 *T. gondii* (moi = 0.5), fixed at 24 hr postinfection, and stained with rabbit anti-*T. gondii* (Alexa 488, green) or rat anti-Cd11b (Alexa 594, red). Scale bars represent 20 μm.

(E) The number of *T. gondii* parasites per vacuole in WT or KO macrophages at 24 hr postinfection. Indicated values are means ± SD of triplicates. $^{*}p < 0.02$, $^{**}p < 0.04$, $^{***}p < 0.002$.

Data are representative of five (A), three (B), and two (D) independent experiments. Data in (C) and (E) are pooled from three independent experiments in which almost 150 cells and 140 vacuoles were counted, respectively. See also Figure S3.

suggesting that Irg-mediated immunity could be affected by *Gbp*^{chr3} deficiency. To test this possibility, we first analyzed the amount of Irgb6 protein expression in IFN-γ-treated macrophages. Similar amounts of Irgb6 protein were induced in wild-type and *Gbp*^{chr3}-deleted cells upon stimulation by IFN-γ (Figure 6B). Next, we tested the recruitment of Irgb6 to the PV by confocal microscopy. At 6 hr postinfection, Irgb6 was detectable at the PV in wild-type cells. In contrast, the recruitment of Irgb6 was severely impaired in *Gbp*^{chr3}-deleted macrophages (Figure 6C). The extent of Irgb6 recruitment was analyzed at 2, 4, and 6 hr postinfection. Compared with that in wild-type cells, the percentage of Irgb6-positive parasites in *Gbp*^{chr3}-deleted cells was significantly lower at every time point analyzed (Figure 6D). In addition to Irgb6, we tested the recruitment of other Irgs such as Irgb10, Irga6, and Irgm3 (Figure S5). The recruitment of Irgb10 to the PV was also impaired in *Gbp*^{chr3}-deleted cells (Figure S5A), whereas that of Irga6 was comparable between wild-type and *Gbp*^{chr3}-deleted cells (Figures S5B and S5C). We failed to observe the accumulation of Irgm3 to the PVs even in IFN-γ-stimulated wild-type cells (data not shown). Taken together, these results suggest that Gbp^{chr3} are required for recruitment of Irgb6 and Irgb10 to the PV of *T. gondii* in IFN-γ-activated macrophages.

Gbps Interact with Irgb6

In a previous study, an overexpressed green fluorescent protein (GFP)-Gbp1 fusion protein was shown to colocalize with endogenous Irgb6 and *T. gondii* parasites (Virreira Winter et al., 2011). We confirmed these observations with endogenous proteins by costaining for anti-Gbp1-5 and anti-Irgb6 in wild-type macrophages infected with *T. gondii* (Figure 6E). Furthermore, intensity profile analysis revealed that the signals for both proteins were detected at almost the same sites (Figure 6F). Then, we assessed the interaction between Gbps and Irgb6 in endogenous settings. Immunoprecipitation with anti-Gbp1-5 coprecipitated Irgb6 in IFN-γ-stimulated macrophages, and the amount of Irgb6 coimmunoprecipitated was markedly increased upon *T. gondii* infection (Figure 6G). These results suggest that the

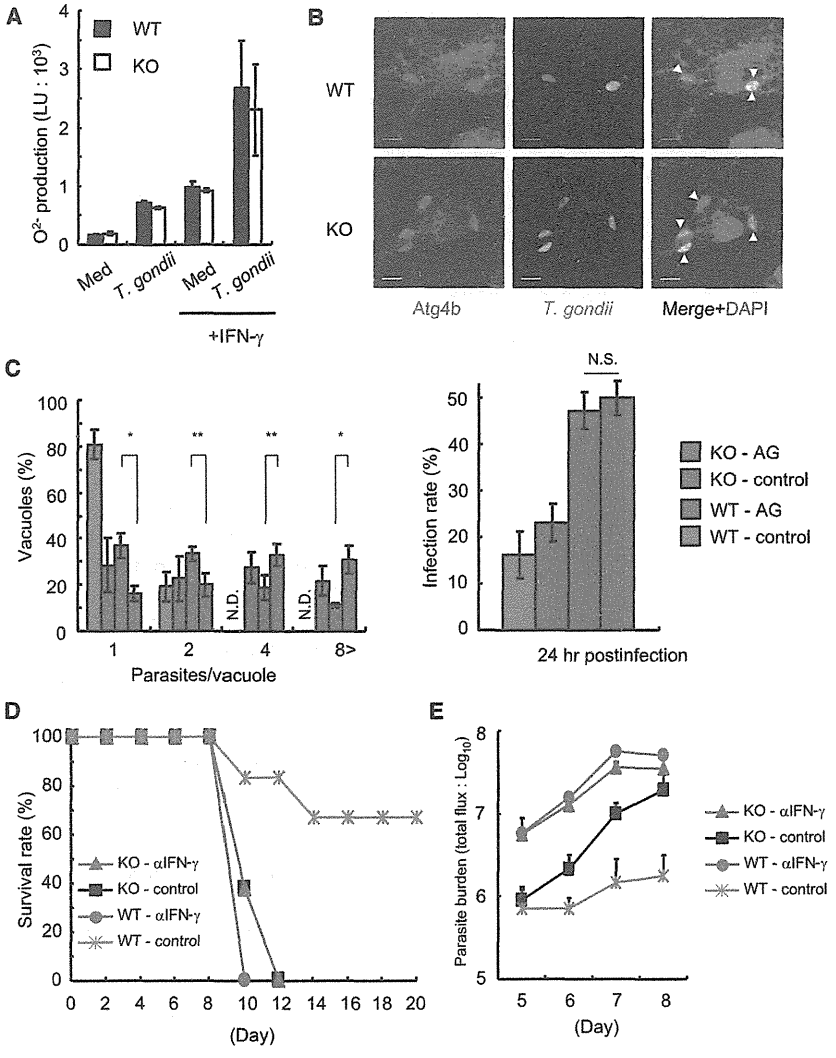

Figure 4. Assessment of IFN-γ-Dependent Responses in *Gbp*^{chr3}-Deleted Mice

(A) Wild-type (WT) and *Gbp*^{chr3}-deleted (KO) peritoneal macrophages were treated with 100 ng/ml IFN-γ for 24 hr. Untreated or IFN-γ-treated cells were uninfected or infected with ME49 *T. gondii* (moi = 0.5) for 24 hr. Concentration (light unit; LU) of O^{2-} in cells was measured with an O^{2-}-specific chemiluminescence reagent by luminometer. Indicated values are means ± SD of triplicates.

(B) WT and KO peritoneal macrophages were treated with 100 ng/ml IFN-γ for 24 hr. IFN-γ-treated cells were infected with ME49 *T. gondii* (moi = 0.5), fixed at 6 hr postinfection, and stained with mouse anti-*T. gondii* (Alexa 488, green) or rabbit anti-Atg4b (Alexa 594, red). Scale bars represent 5 μm.

(C) WT and KO peritoneal macrophages were untreated or treated with 100 ng/ml IFN-γ for 24 hr in the presence or absence of 100 μM AG. Cells were infected with ME49 *T. gondii* expressing luciferase (moi = 0.5). Left: The number of parasites per vacuole in WT or KO macrophages at 24 hr postinfection is shown. Indicated values are means ± SD of triplicates. *$p < 0.01$, **$p < 0.03$. Right: The percentage of WT and KO macrophages containing at least one parasite at 24 hr postinfection is shown. Indicated values are means ± SD of triplicates. N.S., not significant.

(D) Mice (WT intraperitoneally injected with 1 mg of anti-IFN-γ [n = 5] or with control IgG [n = 6] and KO with anti-IFN-γ [n = 8] or with control IgG [n = 8] before 1 day of the parasite challenge) were intraperitoneally infected with 1 × 10^2 *T. gondii*, and the survival rates were monitored for 20 days.

(E) Total photon emission analysis from indicated mice (n = 4 per group) infected with 1 × 10^2 ME49 *T. gondii* luciferase-expressing parasites at days 5, 6, 7, or 8 after infection. The flux (photons/s/cm^2/sr) was determined as a measure of parasite burden.

Data are representative of two (A, B, C, E) independent experiments. Data in (D) are pooled from two independent experiments. See also Figure S4.

association of Irgb6 with Gbps is fundamental to the defective Irgb6 recruitment to *T. gondii* in *Gbp*^{chr3}-deleted cells.

Gbp^{chr3} Participate Differentially in Anti-*T. gondii* Defense

Although the Gbps share a high degree of homology (Kresse et al., 2008), variation in the amino acid sequence among Gbp^{chr3} is greater than that among Gbp^{chr5}. It is uncertain whether the five active members of *Gbp*^{chr3} (*Gbp1*, *Gbp2*, *Gbp3*, *Gbp5*, and *Gbp7*) similarly or differentially contribute to the anti-*T. gondii* cellular immunity. To address this question, we cloned each Gbp into drug-responsive retroviral expression vectors and expressed them in a tightly doxycycline-dependent manner in *Gbp*^{chr3}-deleted primary MEFs (Figure 7A). Parasite clearance in the absence or presence of IFN-γ was then tested in these transduced cells. Reintroduction of *Gbp1*, *Gbp5*, or *Gbp7* into *Gbp*^{chr3}-deleted MEFs *partially* restored the IFN-γ-dependent clearance of *T. gondii* compared with wild-type cells (Figures 3B and 7B), indicating that these proteins possess common and compensatory functions in the anti-*T. gondii* immune response. Taken together, our results show that Gbp^{chr3} play a pivotal role in IFN-γ-mediated cellular innate immune response to *T. gondii*.

DISCUSSION

This study makes use of targeted chromosome engineering to provide genetic evidence for the critical role of Gbp^{chr3} in defense against *T. gondii* infection. Mice lacking *Gbp*^{chr3} were highly susceptible to *T. gondii* infection, and *Gbp*^{chr3}-deleted macrophages are defective in IFN-γ-mediated inhibition of intracellular parasite growth.

The Gbp-mediated cellular immune mechanism was previously reported to be pleiotropic and implicated IFN-γ-inducible phagocytic oxidative killing and the trafficking of antimicrobial peptides to autophagolysosomes by their interaction with NADPH oxidase subunits and autophagy-related molecules such as Atg4b, respectively (Kim et al., 2011). In this previous

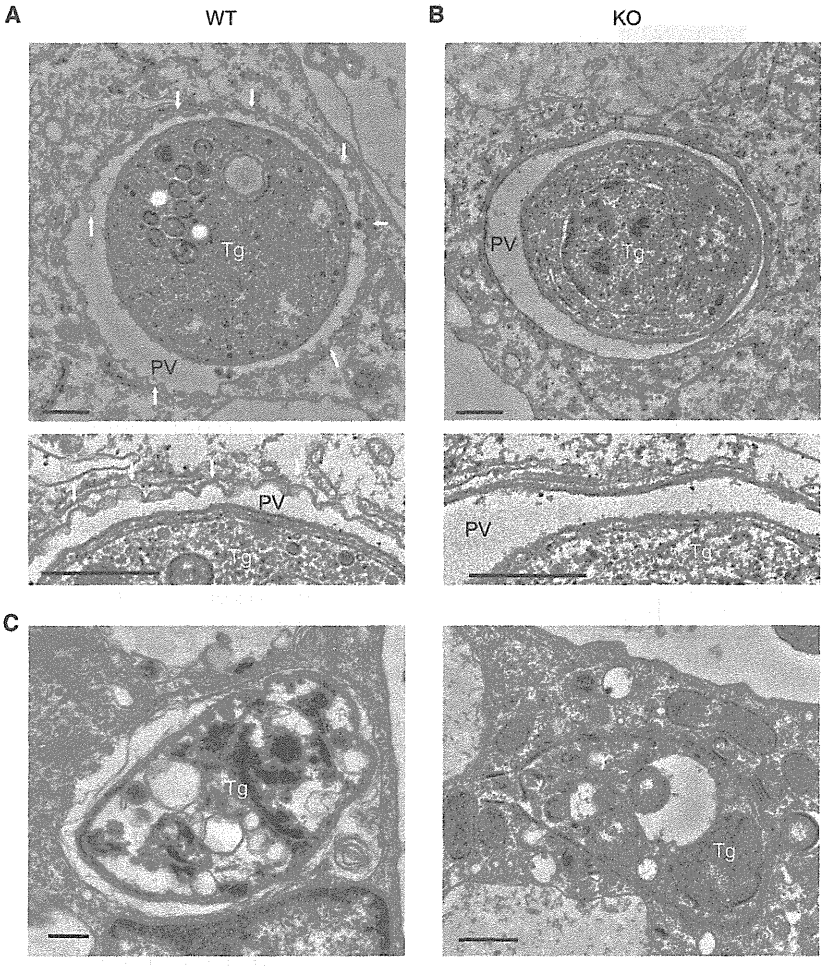

Figure 5. Electron Microscopic Analysis of IFN-γ-Activated Macrophages

(A and B) Wild-type (A) or *Gbp*^{chr3}-deleted (B) peritoneal macrophages were treated with 100 ng/ml IFN-γ for 24 hr. IFN-γ-treated cells were infected with ME49 *T. gondii* (moi = 0.5) for 6 hr and then analyzed by electron microscopy. The lower images are enlarged views from the upper images. Tg, *T. gondii*; PV, parasitophorous vacuole. Arrows indicate protrusive blebs inside or outside parasitophorous vacuoles (A).

(C) Images of dead parasites at 24 hr postinfection in IFN-γ-treated wild-type cells. Tg, *T. gondii*.

Scale bars represent 0.2 μm. Data are representative of two independent experiments.

study, Gbp function was mainly tested with dominant-negative forms of Gbps or small interfering RNA-mediated knockdown (Kim et al., 2011). Here, we observed normal O^{2-} production in response to IFN-γ stimulation and Atg4b recruitment to PVs in *Gbp*^{chr3}-deleted macrophages. Instead, we found that *Gbp*^{chr3} deficiency affected recruitment of some Irgs to *T. gondii*-infected macrophages. The discrepancy between the two studies might be explained by the different pathogens, or alternatively, it is possible that the other cluster of *Gbp*s on chromosome 5 (*Gbp*^{chr5}) may play a compensatory role in the oxidative and autophagy-related responses.

Blebbing of the PV membrane was not induced in IFN-γ-activated macrophages lacking *Gbp*^{chr3}, which is akin to that observed in Atg5-deficient cells (Zhao et al., 2008). The similar phenotypes of both mutant mice prompted us to examine the localization of Irgs during *T. gondii* infection. *Gbp*^{chr3} deficiency impaired accumulation of Irgb6 and Irgb10 but not of Irga6 around the parasite, suggesting that the Gbps play a major role in some Irg recruitment. This model contrasts with previous studies suggesting that Irgs control localization of Gbps based on the fact that IFN-γ prestimulation is required for the localization of overexpressed Gbps to *T. gondii* (Degrandi et al., 2007), and that Gbp2 localization is altered in Irgm-deficient cells (Traver et al., 2011). Considering that Gbps and Irgs participate in the anti-*T. gondii* response in close proximity, it is possible that the two families of IFN-γ-inducible GTPases mutually control their localization, at least in part, through physical association. Given that the number of IRGs and GBPs varies among species (2 IRGs and 7 GBPs in human versus 23 Irgs and 13 Gbps in mouse) (Kresse et al., 2008; Shenoy et al., 2007), evolutionary pressure to increase or decrease the number and variety of IRGs could influence the repertoire of GBPs. Furthermore, virulent *T. gondii* strains such as RH are capable of evading recognition by Irgs via the action of the virulence factor ROP18 that phosphorylates the Irgs (Degrandi et al., 2007; Fentress et al., 2010; Steinfeldt et al., 2010; Virreira Winter et al., 2011). In addition, virulent *T. gondii* also prevents the accumulation of Gbps (Virreira Winter et al., 2011). Taken together, ROP18 phosphorylation of Irgs could affect the interaction with Gbps, promoting their dissociation from the parasites. In terms of the kinetics of the recruitment of Irgb6, given that *Gbp*^{chr3} deficiency affected the later phase rather than the early stage, Gbp^{chr3} might play a role in persistence of Irgb6 on PVs in the later stage. Alternatively, other factors including Gbp^{chr5} might also participate in the Irgb6 recruitment in the early phase of infection. Whether deficiency of either *Gbp*^{chr3} or *Gbp*^{chr5} (or both) also affects the localization of other Irgs such as Irgm and Irgd deserves further investigation. Despite the fact that Irgb6 and Irgb10 are shown to be phosphorylated by ROP18 in vitro (strongly indicating the defensive roles of these Irgs) (Fentress et al., 2010), their in vivo functions in immunity to *T. gondii* should still be assessed and confirmed under physiological conditions via mice lacking these Irgs.

The impaired inhibition of *T. gondii* replication in *Gbp*^{chr3}-deleted cells prompted us to investigate the effect of NO on the *Gbp*^{chr3}-dependent resistance to *T. gondii* in vitro. We found that the presence or absence of NO did not affect parasite clearance; the rate of macrophages infected with *T. gondii* was not altered by addition of the NO inhibitor. Given the collaboration

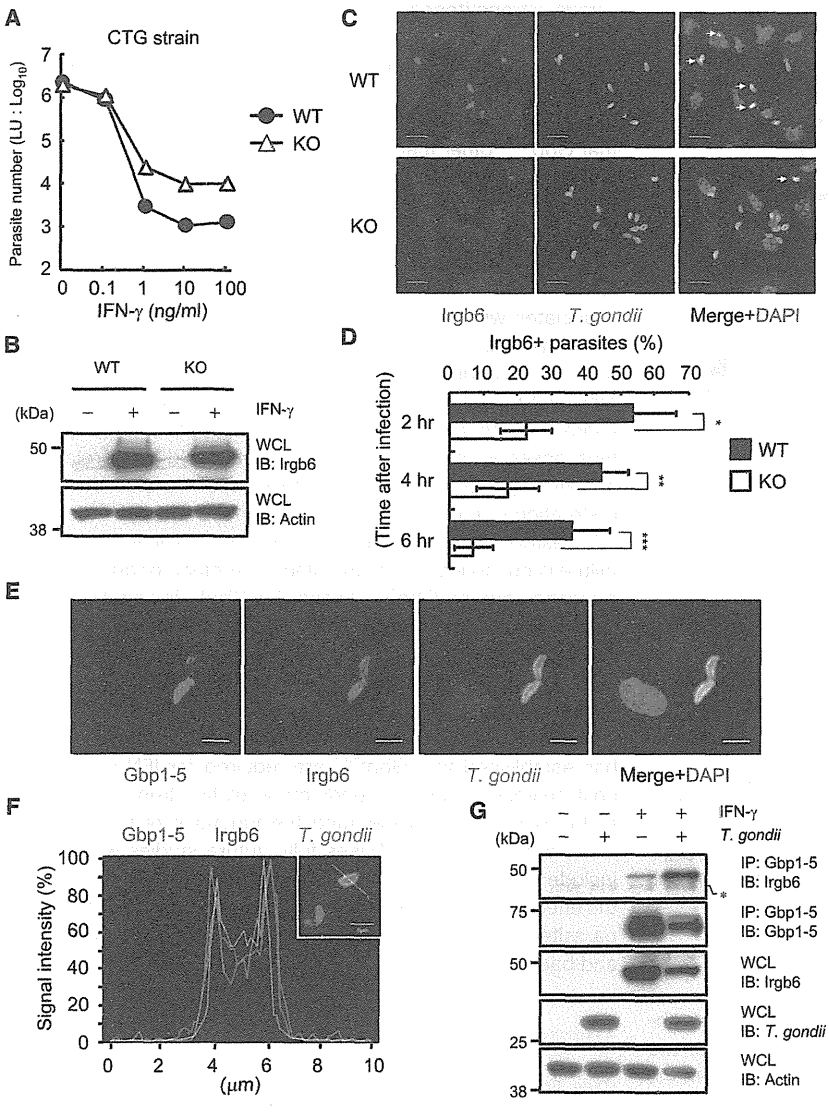

Figure 6. Defective Irgb6 Recruitment in *Gbp*^{chr3}-Deleted Macrophages

(A) Wild-type (WT) and *Gbp*^{chr3}-deleted (KO) peritoneal macrophages were untreated or treated with the indicated concentrations of IFN-γ for 24 hr. Untreated or IFN-γ-treated cells were infected with CTG *T. gondii* expressing luciferase (moi = 0.5) and harvested at 36 hr postinfection. The luciferase units (LU) were assayed with the lysates. Indicated values are means ± SD of triplicates.

(B) Peritoneal macrophages treated with 100 ng/ml IFN-γ for 24 hr were lysed. The lysates were detected by protein immunoblot with the indicated Abs.

(C) WT and KO peritoneal macrophages were treated with 100 ng/ml IFN-γ for 24 hr. IFN-γ-treated cells were infected with ME49 *T. gondii* (moi = 0.5), fixed at 6 hr postinfection, and incubated with rabbit anti-*T. gondii* (Alexa 488, green) or goat anti-Irgb6 (Alexa 594, red). Scale bars represent 10 μm. Arrows indicate colocalization of Irgb6 with *T. gondii*.

(D) The percentage of WT and KO macrophages positive for Irgb6 staining at the indicated points postinfection. Indicated values are means ± SD of triplicates. *p < 0.03, **p < 0.005, ***p < 0.004.

(E and F) Peritoneal macrophages were treated with 100 ng/ml IFN-γ for 24 hr. IFN-γ-treated cells were infected with ME49 *T. gondii* (moi = 0.5), fixed at 6 hr postinfection, and incubated with rabbit anti-*T. gondii* (Alexa 488, green), goat anti-Irgb6 (Alexa 594, red), or mouse anti-Gbp1-5 (Alexa 647, magenta). The samples were analyzed by confocal microscopy and subsequent intensity profile (F). Scale bars represent 5 μm. The signal intensities of each color on the 10 μm white line on the parasites are shown.

(G) Peritoneal macrophages treated with 100 ng/ml IFN-γ for 24 hr were lysed. The lysates were immunoprecipitated with anti-Gbp1-5 and detected by protein immunoblot with the indicated antibodies. Asterisk indicates nonspecific.

Data are representative of two (A, B) or three (C, D, E, F, G) independent experiments. Data in (D) are pooled from three independent experiments, in which almost 150 cells at each time point were counted. See also Figure S5.

of Irg and Gbp, the NO-independent role of Gbp^{chr3} may be parallel to the NO-independent effect of Irg on *T. gondii* clearance (Collazo et al., 2002). In contrast, the presence of Gbp^{chr3} had a modest effect on the inhibition of *T. gondii* replication, which critically involves NO, because *Gbp*^{chr3}-deleted macrophages contained larger numbers of the parasites per PV. Because there is no direct evidence indicating a role of Irg in the suppression of *T. gondii* replication to date, these data may be indicative of an unknown Irg-independent mechanism(s) of Gbp^{chr3} to promote the NO-mediated inhibition of the parasite replication in vitro. Nevertheless, considering that iNOS deficiency has a minor effect on early resistance in vivo (Scharton-Kersten et al., 1997), the high susceptibility in acute *T. gondii* infection in *Gbp*^{chr3}-deleted mice might be due to the defective parasite clearance dependent on some Irgs. Given the relative significance of Gbp^{chr3} in IFN-γ-dependent anti-*T. gondii* responses, the fact that anti-IFN-γ treatment in *Gbp*^{chr3}-deleted mice resulted in enhanced parasite burdens in vivo suggests that additional IFN-γ-inducible effector(s) controls early resistance to the parasite. On the other hand, *Gbp*^{chr3}-deleted mice treated with anti-IFN-γ displayed similar survival rate of mice with control IgG. The apparent disparity might be because anti-IFN-γ blocked IFN-γ-dependent anti-*T. gondii* response, leading not only to high parasite burdens but also to immune pathology mediated by massive and dysregulated doses of IFN-γ at the terminal phase of *T. gondii* infection (Nguyen et al., 2003). In addition, costimulation of TNF-α with IFN-γ resulted in incomparable inhibition of the parasite growth and abolished the Gbp^{chr3}-mediated effect. Although NO concentration in TNF-α and IFN-γ-treated macrophages was markedly higher than that in cells stimulated with IFN-γ alone, further investigation is required to determine whether only the difference of NO

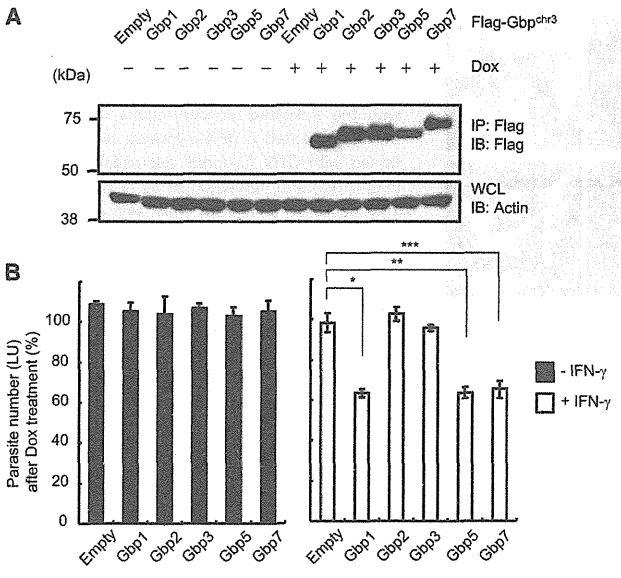

Figure 7. Individual Participation of Gbp^{chr3} in IFN-γ-Dependent Inhibition of *T. gondii* Growth

(A) Retroviral vectors encoding the indicated Flag-tagged Gbps were stably introduced in *Gbp*^{chr3}-deleted (KO) primary MEFs. The transfected MEFs were treated with or without 1 μg/ml doxycycline (Dox) for 24 hr and lysed. The lysates were immunoprecipitated with anti-Flag and detected by protein immunoblot with the indicated antibodies.

(B) The KO MEFs transfected with indicated Gbps were unstimulated or stimulated with 100 ng/ml of IFN-γ for 24 hr with or without 1 μg/ml Dox. Cells were infected with ME49 *T. gondii* parasites expressing luciferase (moi = 0.5) for 36 hr, and the luciferase units (LU) were analyzed. The percentages of the activities after each Gbp induction with Dox over those without Dox (no Gbp induction) in nonstimulated (left) or stimulated (right) cells were shown. Indicated values are means ± SD of triplicates.

Data are representative of two independent experiments. *, **, ***$p < 0.001$.

concentration or other NO-independent effects such as autophagy and augmentation of phagocytic activity accounts for the enhanced protective effect (Keller et al., 2011; Langermans et al., 1992; Leenen et al., 1994).

Gbp1, Gbp5, and Gbp7, but not Gbp2 or Gbp3, were able to restore, albeit not fully, the killing activity by IFN-γ in *Gbp*^{chr3}-deleted MEFs, indicating that Gbp^{chr3} contribute differentially to the anti-*T. gondii* host defense mechanism. This is consistent with a previous finding that knockdown of some Gbps abrogates IFN-γ-dependent suppression of bacterial growth (Kim et al., 2011). In the context of the functional redundancy within Gbp^{chr3}, we observed that mice lacking *Gbp5*, or *Gbp5* and *Gbp2ps*, were resistant to *T. gondii* infection, suggesting that *Gbp5* deficiency may be compensated for by other *Gbp*^{chr3}-encoded proteins such as Gbp1 and Gbp7. On the other hand, mice lacking Gbp1 alone are susceptible to *L. monocytogenes* and *M. bovis*. Interestingly, Gbp5 has recently been shown to play a key role in the host defense in *L. monocytogenes* infection, indicating the nonredundant function of Gbp1 and Gbp5 in the antibacterial response (Kim et al., 2011; Shenoy et al., 2012). In contrast, our *Gbp*^{chr3}-deleted mice displayed resistance to *L. monocytogenes*. This discrepancy may reflect different modes of infection (e.g., oral versus intraperitoneal infections in the previous and current studies, respectively) or utilization of different mice strains (*Gbp1* or *Gbp5* singly deficient mice in previous studies and *Gbp*^{chr3}-deleted mice in this study) (Kim et al., 2011; Shenoy et al., 2012). Moreover, we could not exclude the possibility that Gbp^{chr3} other than *Gbp1* and *Gbp5* play a negative role in Gbp1- and Gbp5-mediated anti-*Listeria* response. It remains to be seen whether deficiency of Gbp1 alone would be sufficient to disrupt the anti-*T. gondii* defense system, but it is nevertheless plausible that each member of Gbp^{chr3} may play a differential role to combat distinct types of pathogens. Given that Gbp2 associates with Gbp1 (Virreira Winter et al., 2011), Gbp2 (and Gbp3) might play a role in host defense against other pathogens or have an additional anti-*T. gondii* effect in the presence of other Gbp^{chr3}. Considering that *Gbp*^{chr3}-deleted cells lack a large genetic region, there is an inherant risk that the phenotype observed in *Gbp*^{chr3}-deleted mice could be unrelated to Irg. Although we adopted in vitro retroviral transfection for the restoration of each Gbp in this study, none of Gbp^{chr3} failed to fully restore the effect of IFN-γ. It remains unclear whether the failure is due to limit of the transfection method or due to nonredundancy among Gbp^{chr3} except for Gbp5. In vivo transgenic reconstitution of the region by an artificial chromosome such as BAC and YAC should be utilized to reveal a role of each Gbp specifically participating in antiparasite in vivo responses in the future (Copeland et al., 2001).

In conclusion, our genetic study with *Gbp*^{chr3}-deleted mice has established that Gbp^{chr3} are required for IFN-γ-mediated host defense against *T. gondii* by regulating Irgb6 recruitment to the parasite. To understand the functions of this family of IFN-γ-inducible p65 GTPases fully, future studies will have to include the second cluster, Gbp^{chr5}, and will need to investigate the effect of these proteins in defense against a broader range of parasites, as well as against other pathogens including viruses and bacteria.

EXPERIMENTAL PROCEDURES

Cells, Mice, and Parasites

C57BL/6 mice were obtained from SLC. ME49 and CTG derivatives of *T. gondii* were maintained in Vero cells by biweekly passage in RPMI1640 (Nacalai Tesque) supplemented with 2% heat-inactivated fetal calf serum (JRH Bioscience), 100 U/ml penicillin, and 0.1 mg/ml streptomycin (GIBCO). MyD88-deficient mice were kindly provided by S. Akira. Animal experiments were conducted with the approval of the Animal Research Committee of the Graduate School of Medicine and of the Research Institute for Microbial Diseases, Osaka University.

Reagents

Antibodies against *T. gondii* (sc-73210), TGTP (Irgb6; sc-11079), Atg4b (sc-130968), Gbp1 (sc-10586), Gbp2 (sc-10588), Gbp5 (sc-160356), Gbp1-5 (sc-166960), and actin (sc-8432) were purchased from Santa Cruz. Anti-CD11b (M1/70) was obtained from Becton Dickinson. Aminoguanidine hydrochloride, LPS (a TLR4 ligand) from *Salmonella minnesota* Re 595, and anti-Flag were purchased from Sigma. Anti-GAP45 rabbit and anti-MIC2 mouse antibodies were as described previously (Frénal et al., 2010). Anti-Irga6 (165/3) and Irgb10 (940/6) rabbit antibodies and anti-Irgm3 (BD Transduction Laboratories) mouse antibodies were kindly provided by J. Howard. Anti-IFN-γ (BE0055) and control Rat IgG1 (BE0088) were obtained from BioXcell. Recombinant IFN-γ and TNF-α were obtained from Peprotech.

In Vivo Measurement of Parasites by Imaging

Mice were intraperitoneally infected with 1×10^2 freshly egressed ME49 tachyzoites expressing luciferase resuspended in 100 μl PBS, and bioluminescence was assessed on the indicated days after infection. Treatment of anti-IFN-γ and control IgG was performed by the intraperitoneal injection 1 day before *T. gondii* infection. For the detection of bioluminescence emission, mice were intraperitoneally injected with 3 mg of D-luciferin in 200 μl PBS (Promega), maintained for 5 min to allow adequate dissemination of the luciferin, then anesthetized with isoflurane (Dainippon Sumitomo Pharma). At 10 min postinjection of D-luciferin, abdominal photon emission was assessed during a 60 s exposure by an in vivo imaging system (IVIS 100; Xenogen) and analyzed as described previously (Yamamoto et al., 2011).

Immunofluorescence

Peritoneal macrophages (1×10^6) infected with *T. gondii* (moi = 0.5) were fixed for 10 min in PBS containing 3.7% formaldehyde. Cells were permeabilized with PBS containing 0.1% Triton X-100 and then blocked with 8% fetal calf serum in PBS. Subsequently, cells were incubated with anti-CD11b rat antibody (1:200) and anti-GAP45 rabbit antibody (1:1,000) in Figure 3D; anti-Atg4b rabbit antibody (1:200) and anti-*T. gondii* mouse antibody (1:50) in Figure 4B; anti-GAP45 rabbit antibody (1:1,000), anti-Irgb6 goat antibody (1:50), and anti-Gbp1-5 mouse antibody (1:200) in Figure 6; and anti-Irgb10 or anti-Irga6 rabbit antibody (1:1,000) and anti-MIC2 mouse antibody (1:1,000), anti-Irgm3 mouse antibody (1:250), and anti-GAP45 rabbit antibody (1:1,000) in Figure S5, for 1 hr at 37°C, followed by incubation with donkey IgG antibodies (1:10,000): Alexa Fluor 488-conjugated anti-rabbit IgG, Alexa Fluor 594-conjugated anti-goat, or Alexa Fluor 647 or Alexa Fluor 594-conjugated anti-mouse (Molecular Probes) for 1 hr at room temperature in the dark. Finally, the immunostained cells were mounted with PermaFluor (Thermo Scientific) on glass slides and analyzed by confocal laser microscopy (FV1000-D IX-81; Olympus); the images were analyzed with Fluoview (Olympus).

Transmission Electron Microscopy

Peritoneal macrophages (1×10^6) untreated or treated with 100 ng/ml IFN-γ for 24 hr were infected with *T. gondii* (moi = 0.5) for 6 or 24 hr. After washing with PBS, the cells were fixed with 2.5% glutaraldehyde in 0.1 M phosphate buffer at 4°C overnight. The cells were postfixed with 1% OsO_4 in the same buffer at 4°C for 1 hr, dehydrated in a graded series of ethanol, and embedded in Quetol 812 (Nissin EM). Silver sections were cut with an ultramicrotome, stained with lead citrate and uranyl acetate, and observed with an H-7650 electron microscope (Hitachi).

Statistical Analysis

The unpaired Student's t test was used to determine the statistical significance of the experimental data.

SUPPLEMENTAL INFORMATION

Supplemental Information includes Supplemental Experimental Procedures, five figures, and one table and can be found with this article online at http://dx.doi.org/10.1016/j.immuni.2012.06.009.

ACKNOWLEDGMENTS

We thank C. Hidaka for excellent secretarial assistance, Y. Magota and M. Enomoto for technical assistance, and members of K.T.'s lab for discussions. Rabbit anti-Irgb6 and Irgb10 and mouse anti-Irgm3 were kindly provided by J.C. Howard. This work was supported by grants from the Ministry of Education, Culture, Sports, Science and Technology; Kanae Foundation for the Promotion of Medical Science; The Cell Science Research Foundation; Kato Memorial Bioscience Foundation; The Uehara Memorial Foundation; Naito Foundation; Mochida Memorial Foundation for Medical and Pharmaceutical Research; The Waksman Foundation of Japan Inc.; Senri Life Science Foundation; The Tokyo Biochemical Research Foundation; The Research Foundation for Microbial Diseases of Osaka University; The Nakajima Foundation; The Asahi Glass Foundation; and The Osaka Foundation for Promotion of Clinical Immunology. M.Y. and D.S.-F. are supported by the Japanese-Swiss bilateral program of The Strategic International Cooperative Program (Research Exchange Type), the Japan Science and Technology Agency (JST).

Received: February 8, 2012
Revised: April 23, 2012
Accepted: June 11, 2012
Published online: July 12, 2012

REFERENCES

Adams, L.B., Hibbs, J.B., Jr., Taintor, R.R., and Krahenbuhl, J.L. (1990). Microbiostatic effect of murine-activated macrophages for *Toxoplasma gondii*. Role for synthesis of inorganic nitrogen oxides from L-arginine. J. Immunol. *144*, 2725–2729.

Aliberti, J., Valenzuela, J.G., Carruthers, V.B., Hieny, S., Andersen, J., Charest, H., Reis e Sousa, C., Fairlamb, A., Ribeiro, J.M., and Sher, A. (2003). Molecular mimicry of a CCR5 binding-domain in the microbial activation of dendritic cells. Nat. Immunol. *4*, 485–490.

Boehm, U., Klamp, T., Groot, M., and Howard, J.C. (1997). Cellular responses to interferon-gamma. Annu. Rev. Immunol. *15*, 749–795.

Boothroyd, J.C. (2009). *Toxoplasma gondii*: 25 years and 25 major advances for the field. Int. J. Parasitol. *39*, 935–946.

Boothroyd, J.C., and Dubremetz, J.F. (2008). Kiss and spit: the dual roles of *Toxoplasma rhoptries*. Nat. Rev. Microbiol. *6*, 79–88.

Collazo, C.M., Yap, G.S., Sempowski, G.D., Lusby, K.C., Tessarollo, L., Woude, G.F., Sher, A., and Taylor, G.A. (2001). Inactivation of LRG-47 and IRG-47 reveals a family of interferon gamma-inducible genes with essential, pathogen-specific roles in resistance to infection. J. Exp. Med. *194*, 181–188.

Collazo, C.M., Yap, G.S., Hieny, S., Caspar, P., Feng, C.G., Taylor, G.A., and Sher, A. (2002). The function of gamma interferon-inducible GTP-binding protein IGTP in host resistance to *Toxoplasma gondii* is Stat1 dependent and requires expression in both hematopoietic and nonhematopoietic cellular compartments. Infect. Immun. *70*, 6933–6939.

Copeland, N.G., Jenkins, N.A., and Court, D.L. (2001). Recombineering: a powerful new tool for mouse functional genomics. Nat. Rev. Genet. *2*, 769–779.

Degrandi, D., Konermann, C., Beuter-Gunia, C., Kresse, A., Würthner, J., Kurig, S., Beer, S., and Pfeffer, K. (2007). Extensive characterization of IFN-induced GTPases mGBP1 to mGBP10 involved in host defense. J. Immunol. *179*, 7729–7740.

Deretic, V. (2006). Autophagy as an immune defense mechanism. Curr. Opin. Immunol. *18*, 375–382.

Fentress, S.J., Behnke, M.S., Dunay, I.R., Mashayekhi, M., Rommereim, L.M., Fox, B.A., Bzik, D.J., Taylor, G.A., Turk, B.E., Lichti, C.F., et al. (2010). Phosphorylation of immunity-related GTPases by a *Toxoplasma gondii*-secreted kinase promotes macrophage survival and virulence. Cell Host Microbe *8*, 484–495.

Frénal, K., Polonais, V., Marq, J.B., Stratmann, R., Limenitakis, J., and Soldati-Favre, D. (2010). Functional dissection of the apicomplexan glideosome molecular architecture. Cell Host Microbe *8*, 343–357.

Gorbacheva, V.Y., Lindner, D., Sen, G.C., and Vestal, D.J. (2002). The interferon (IFN)-induced GTPase, mGBP-2. Role in IFN-gamma-induced murine fibroblast proliferation. J. Biol. Chem. *277*, 6080–6087.

Guenzi, E., Töpolt, K., Cornali, E., Lubeseder-Martellato, C., Jörg, A., Matzen, K., Zietz, C., Kremmer, E., Nappi, F., Schwemmle, M., et al. (2001). The helical domain of GBP-1 mediates the inhibition of endothelial cell proliferation by inflammatory cytokines. EMBO J. *20*, 5568–5577.

Guenzi, E., Töpolt, K., Lubeseder-Martellato, C., Jörg, A., Naschberger, E., Benelli, R., Albini, A., and Stürzl, M. (2003). The guanylate binding protein-1 GTPase controls the invasive and angiogenic capability of endothelial cells through inhibition of MMP-1 expression. EMBO J. *22*, 3772–3782.

Howard, J.C., Hunn, J.P., and Steinfeldt, T. (2011). The IRG protein-based resistance mechanism in mice and its relation to virulence in *Toxoplasma gondii*. Curr. Opin. Microbiol. *14*, 414–421.

Hunter, C.A., and Remington, J.S. (1995). The role of IL12 in toxoplasmosis. Res. Immunol. *146*, 546–552.

Hunter, C.A., Candolfi, E., Subauste, C., Van Cleave, V., and Remington, J.S. (1995). Studies on the role of interleukin-12 in acute murine toxoplasmosis. Immunology *84*, 16–20.

Israelski, D.M., and Remington, J.S. (1993). Toxoplasmosis in patients with cancer. Clin. Infect. Dis. *17* (*Suppl 2*), S423–S435.

Jensen, K.D., Wang, Y., Wojno, E.D., Shastri, A.J., Hu, K., Cornel, L., Boedec, E., Ong, Y.C., Chien, Y.H., Hunter, C.A., et al. (2011). Toxoplasma polymorphic effectors determine macrophage polarization and intestinal inflammation. Cell Host Microbe *9*, 472–483.

Keller, C.W., Fokken, C., Turville, S.G., Lünemann, A., Schmidt, J., Münz, C., and Lünemann, J.D. (2011). TNF-alpha induces macroautophagy and regulates MHC class II expression in human skeletal muscle cells. J. Biol. Chem. *286*, 3970–3980.

Kim, B.H., Shenoy, A.R., Kumar, P., Das, R., Tiwari, S., and MacMicking, J.D. (2011). A family of IFN-γ-inducible 65-kD GTPases protects against bacterial infection. Science *332*, 717–721.

Kresse, A., Konermann, C., Degrandi, D., Beuter-Gunia, C., Wuerthner, J., Pfeffer, K., and Beer, S. (2008). Analyses of murine GBP homology clusters based on in silico, in vitro and in vivo studies. BMC Genomics *9*, 158.

Langermans, J.A., Van der Hulst, M.E., Nibbering, P.H., Hiemstra, P.S., Fransen, L., and Van Furth, R. (1992). IFN-gamma-induced L-arginine-dependent toxoplasmastatic activity in murine peritoneal macrophages is mediated by endogenous tumor necrosis factor-alpha. J. Immunol. *148*, 568–574.

Leenen, P.J., Canono, B.P., Drevets, D.A., Voerman, J.S., and Campbell, P.A. (1994). TNF-alpha and IFN-gamma stimulate a macrophage precursor cell line to kill *Listeria monocytogenes* in a nitric oxide-independent manner. J. Immunol. *153*, 5141–5147.

Li, M., Mukasa, A., Inda, Md., Zhang, J., Chin, L., Cavenee, W., and Furnari, F. (2011). Guanylate binding protein 1 is a novel effector of EGFR-driven invasion in glioblastoma. J. Exp. Med. *208*, 2657–2673.

Ling, Y.M., Shaw, M.H., Ayala, C., Coppens, I., Taylor, G.A., Ferguson, D.J., and Yap, G.S. (2006). Vacuolar and plasma membrane stripping and autophagic elimination of *Toxoplasma gondii* in primed effector macrophages. J. Exp. Med. *203*, 2063–2071.

MacMicking, J.D. (2004). IFN-inducible GTPases and immunity to intracellular pathogens. Trends Immunol. *25*, 601–609.

Montoya, J.G., and Remington, J.S. (2008). Management of *Toxoplasma gondii* infection during pregnancy. Clin. Infect. Dis. *47*, 554–566.

Nguyen, T.D., Bigaignon, G., Markine-Goriaynoff, D., Heremans, H., Nguyen, T.N., Warnier, G., Delmee, M., Warny, M., Wolf, S.F., Uyttenhove, C., et al. (2003). Virulent *Toxoplasma gondii* strain RH promotes T-cell-independent overproduction of proinflammatory cytokines IL12 and gamma-interferon. J. Med. Microbiol. *52*, 869–876.

Plattner, F., Yarovinsky, F., Romero, S., Didry, D., Carlier, M.F., Sher, A., and Soldati-Favre, D. (2008). *Toxoplasma* profilin is essential for host cell invasion and TLR11-dependent induction of an interleukin-12 response. Cell Host Microbe *3*, 77–87.

Sadler, A.J., and Williams, B.R. (2008). Interferon-inducible antiviral effectors. Nat. Rev. Immunol. *8*, 559–568.

Saeij, J.P., Boyle, J.P., Coller, S., Taylor, S., Sibley, L.D., Brooke-Powell, E.T., Ajioka, J.W., and Boothroyd, J.C. (2006). Polymorphic secreted kinases are key virulence factors in toxoplasmosis. Science *314*, 1780–1783.

Scharton-Kersten, T.M., Yap, G., Magram, J., and Sher, A. (1997). Inducible nitric oxide is essential for host control of persistent but not acute infection with the intracellular pathogen *Toxoplasma gondii*. J. Exp. Med. *185*, 1261–1273.

Shenoy, A.R., Kim, B.H., Choi, H.P., Matsuzawa, T., Tiwari, S., and MacMicking, J.D. (2007). Emerging themes in IFN-gamma-induced macrophage immunity by the p47 and p65 GTPase families. Immunobiology *212*, 771–784.

Shenoy, A.R., Wellington, D.A., Kumar, P., Kassa, H., Booth, C.J., Cresswell, P., and MacMicking, J.D. (2012). GBP5 promotes NLRP3 inflammasome assembly and immunity in mammals. Science *336*, 481–485.

Sibley, L.D., Adams, L.B., Fukutomi, Y., and Krahenbuhl, J.L. (1991). Tumor necrosis factor-alpha triggers antitoxoplasmal activity of IFN-gamma primed macrophages. J. Immunol. *147*, 2340–2345.

Steinfeldt, T., Könen-Waisman, S., Tong, L., Pawlowski, N., Lamkemeyer, T., Sibley, L.D., Hunn, J.P., and Howard, J.C. (2010). Phosphorylation of mouse immunity-related GTPase (IRG) resistance proteins is an evasion strategy for virulent *Toxoplasma gondii*. PLoS Biol. *8*, e1000576.

Suzuki, Y., Orellana, M.A., Schreiber, R.D., and Remington, J.S. (1988). Interferon-gamma: the major mediator of resistance against *Toxoplasma gondii*. Science *240*, 516–518.

Taylor, G.A., Collazo, C.M., Yap, G.S., Nguyen, K., Gregorio, T.A., Taylor, L.S., Eagleson, B., Secrest, L., Southon, E.A., Reid, S.W., et al. (2000). Pathogen-specific loss of host resistance in mice lacking the IFN-gamma-inducible gene IGTP. Proc. Natl. Acad. Sci. USA *97*, 751–755.

Taylor, G.A., Feng, C.G., and Sher, A. (2004). p47 GTPases: regulators of immunity to intracellular pathogens. Nat. Rev. Immunol. *4*, 100–109.

Taylor, S., Barragan, A., Su, C., Fux, B., Fentress, S.J., Tang, K., Beatty, W.L., Hajj, H.E., Jerome, M., Behnke, M.S., et al. (2006). A secreted serine-threonine kinase determines virulence in the eukaryotic pathogen *Toxoplasma gondii*. Science *314*, 1776–1780.

Taylor, G.A., Feng, C.G., and Sher, A. (2007). Control of IFN-gamma-mediated host resistance to intracellular pathogens by immunity-related GTPases (p47 GTPases). Microbes Infect. *9*, 1644–1651.

Traver, M.K., Henry, S.C., Cantillana, V., Oliver, T., Hunn, J.P., Howard, J.C., Beer, S., Pfeffer, K., Coers, J., and Taylor, G.A. (2011). Immunity-related GTPase M (IRGM) proteins influence the localization of guanylate-binding protein 2 (GBP2) by modulating macroautophagy. J. Biol. Chem. *286*, 30471–30480.

Trinchieri, G. (2003). Interleukin-12 and the regulation of innate resistance and adaptive immunity. Nat. Rev. Immunol. *3*, 133–146.

Virreira Winter, S., Niedelman, W., Jensen, K.D., Rosowski, E.E., Julien, L., Spooner, E., Caradonna, K., Burleigh, B.A., Saeij, J.P., Ploegh, H.L., and Frickel, E.M. (2011). Determinants of GBP recruitment to Toxoplasma gondii vacuoles and the parasitic factors that control it. PLoS ONE *6*, e24434.

Whitmarsh, R.J., Gray, C.M., Gregg, B., Christian, D.A., May, M.J., Murray, P.J., and Hunter, C.A. (2011). A critical role for SOCS3 in innate resistance to *Toxoplasma gondii*. Cell Host Microbe *10*, 224–236.

Yamamoto, M., Ma, J.S., Mueller, C., Kamiyama, N., Saiga, H., Kubo, E., Kimura, T., Okamoto, T., Okuyama, M., Kayama, H., et al. (2011). ATF6β is a host cellular target of the *Toxoplasma gondii* virulence factor ROP18. J. Exp. Med. *208*, 1533–1546.

Yarovinsky, F., and Sher, A. (2006). Toll-like receptor recognition of *Toxoplasma gondii*. Int. J. Parasitol. *36*, 255–259.

Yarovinsky, F., Zhang, D., Andersen, J.F., Bannenberg, G.L., Serhan, C.N., Hayden, M.S., Hieny, S., Sutterwala, F.S., Flavell, R.A., Ghosh, S., and Sher, A. (2005). TLR11 activation of dendritic cells by a protozoan profilin-like protein. Science *308*, 1626–1629.

Zhao, Z., Fux, B., Goodwin, M., Dunay, I.R., Strong, D., Miller, B.C., Cadwell, K., Delgado, M.A., Ponpuak, M., Green, K.G., et al. (2008). Autophagosome-independent essential function for the autophagy protein Atg5 in cellular immunity to intracellular pathogens. Cell Host Microbe *4*, 458–469.

Biochimica et Biophysica Acta 1820 (2012) 1405–1411

Contents lists available at SciVerse ScienceDirect

Biochimica et Biophysica Acta

journal homepage: www.elsevier.com/locate/bbagen

Development of an antibody-lectin enzyme immunoassay for fucosylated α-fetoprotein ☆

Hiroaki Korekane [a,b,c], Tomoko Hasegawa [a], Akio Matsumoto [a,1], Noriaki Kinoshita [d], Eiji Miyoshi [e], Naoyuki Taniguchi [a,b,c,*]

[a] Department of Disease Glycomics (Seikagaku Corporation), The Institute of Scientific and Industrial Research, Osaka University, 8-1 Mihogaoka, Ibaraki, Osaka 567-0047, Japan
[b] RIKEN-ISIR Osaka Univ. Alliance Lab., The Institute of Scientific and Industrial Research, Osaka University, 8-1 Mihogaoka, Ibaraki, Osaka 567-0047, Japan
[c] Disease Glycomics Team, Systems Glycobiology Research Group, Chemical Biology Department, Advanced Science Institute, RIKEN, 2-1 Hirosawa, Wako, Saitama 351-0198, Japan
[d] Immuno-Biological Laboratories Co., Ltd, 1091-1 Naka Aza-Higashida, Fujioka, Gunma 375-0005, Japan
[e] Department of Molecular Biochemistry and Clinical Investigation, Osaka University Graduate School of Medicine, 1-7 Yamadaoka, Suita 565-0871, Japan

ARTICLE INFO

Article history:
Received 18 October 2011
Received in revised form 19 December 2011
Accepted 21 December 2011
Available online 31 December 2011

Keywords:
Antibody-lectin enzyme immunoassay
α-Fetoprotein
Fucosylation
Liver cancer

ABSTRACT

Background: Fucosylation is one of the most important types of glycosylations related to cancer. Our previous studies of the enzymatic basis and structural studies of α-fetoprotein (AFP) samples from liver cancer patients indicated that core-fucosylation by α1,6-fucosyltransferase (FUT8) resulted in the production of fucosylated AFP, and in fact fucosylated AFP allowed differential diagnosis in some types of liver cancer from liver cirrhosis. This served as a predictive biomarker for the development of liver cancer 3 to 18 months before it could be detected using imaging techniques. Fucosylated AFP is currently measured by means of a liquid-phase binding assay (LBA) or by an electrokinetic analyte transport assay (EATA). However, these methods require special instrumentation that is currently available only in major medical laboratories. To overcome this problem, we attempted to develop an enzyme immunoassay (EIA) based on the sandwich technique with specific antibody and lectin.

Results: Dilute solutions of highly fucosylated AFP in human sera were assayed using a microtiter plate coated with a periodate-oxidized anti-AFP antibody, a fucose-specific biotinylated *Aleuria aurantia* lectin (AAL), a peroxidase-conjugated streptoavidin, and a chemiluminescent detection system. The technique was able to measure highly fucosylated AFP diluted to 5 to 80 ng/ml in human sera using the developed antibody-lectin EIA in combination with the enrichment of AFP.

Conclusion: A simple method using an antibody-lectin EIA for quantifying fucosylated AFP that does not require special instrumentation was developed.

General significance: The method can be generally applied to the quantitative measurement of various fucosylated glycoproteins using specific antibodies. This article is part of a Special Issue entitled Glycoproteomics.

1. Introduction

Glycosylation is the most abundant posttranslational modification of proteins [1] and is known to play an important role in the development and progression of various human diseases [2,3]. Aberrant glycosylation occurs in essentially all types of human cancers and a large number of glycosyl epitopes are classified as tumor-associated carbohydrate antigens [4,5]. Some of these tumor-associated carbohydrate antigens have already been utilized as useful tumor biomarkers in the diagnosis of cancers [6]. Subsequent studies shed considerable light on the functional significance of the tumor-associated glycosylation in cancer malignancy, such as metastasis and invasion [6,7]. Thus, the identification of a novel tumor-associated glycosylation should provide important clues concerning the involvement of the glycosylation in cancer malignancy and to develop a potentially useful tumor biomarker.

Alpha-fetoprotein (AFP) is an oncofetal serum glycoprotein that contains a single *N*-glycosylation site at asparagine-232 [8]. It is well-known that the total AFP concentration in human serum is used as a tumor-marker for hepatocellular carcinomas (HCC), but it is sometimes also elevated in benign liver diseases such as chronic hepatitis and liver cirrhosis [9]. In contrast, AFP modified with a core-fucosylation (fucosylated AFP, Fig. 1) is known to be a very specific tumor marker for HCC having a superior specificity and sensitivity compared to the total AFP concentration [10–12] and was

☆ This article is part of a Special Issue entitled Glycoproteomics.

* Corresponding author at: Systems Glycobiology Research Group, Chemical Biology Department, Advanced Science Institute, RIKEN, 2-1 Hirosawa, Wako, Saitama 351-0198, Japan. Tel.: +81 48 467 9616; fax: +81 48 467 9617.
E-mail address: tani52@wd5.so-net.ne.jp (N. Taniguchi).
[1] Present address: Department of Pharmacology, Chiba University Graduate School of Medicine, 1-8-1 Inohana, Chuo-ku, Chiba 260-8670, Japan.

0304-4165/$ – see front matter © 2011 Elsevier B.V. All rights reserved.
doi:10.1016/j.bbagen.2011.12.015

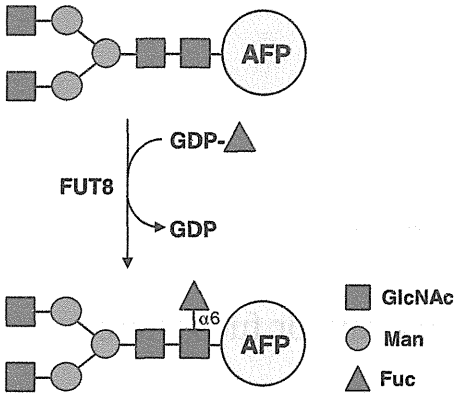

Fig. 1. Schematic representation of the enzymatic basis for the formation of fucosylated AFP. Mammalian α1,6-fucosyltransferase (FUT8), which was purified and its cDNA was cloned by our group, catalyzes the transfer of a fucose residue from the donor substrate, GDP-L-fucose, to the reducing terminal GlcNAc in the *N*-gycans of AFP via an α1,6-linkage (termed as core-fucose) resulting in the formation of fucosylated AFP.

approved as a tumor marker for HCC by the FDA (Food and Drug Administration) in 2005. The fucosylated AFP is an example of one of the most excellent and useful glycoprotein-based tumor biomarkers.

Glycoproteomics is the study of the glycosylation of proteins [13], and its application in the field of cancer would greatly facilitate the identification of candidate glycoprotein biomarkers that have undergone cancer-related glycosylation in a variety of human cancers [14–17]. After the identification of candidate glycoproteins, however, it becomes very important to validate that they are, in fact, biomarkers using large number of clinical samples. In this validation step, the need for a simple, reliable, and high-throughput method to quantitatively determine the candidate glycoprotein biomarkers in clinical samples such as human sera becomes of paramount importance. If it were possible to measure glycoprotein biomarkers using a sandwich technique with an antibody that is specific for the marker and a lectin, this would speed up the validation process and promote clinical applications of the glycoprotein biomarkers. So far, several reports have appeared concerning the development of such assay methods including those against sialylated transferrin [18], fucosylated α_1-acid glycoprotein [19], fucosylated hemopexin [20], and fucosylated haptoglobin [21]. In addition, we also performed previously a pioneering work on the development of such an assay method, designated an antibody-lectin enzyme immunoassay (EIA) for fucosylated AFP [22]. The method involved the use of an anti-AFP antibody, peroxidase-conjugated lectins, and a colorimetric detection system for the characterization of the fucosylation of AFP in various liver diseases, including cancer [22]. We had assumed that the basic technique of an antibody-lectin EIA was established at that time, but subsequent careful evaluation of the assay system revealed several drawbacks, especially in sensitivity and specificity, as detailed below (data not shown). i) The colorimetric detection system used in these studies was not sufficient for detecting AFP at concentrations less than 200 ng/ml. ii) The possibility that contaminated highly-abundant serum glycoproteins were simultaneously assayed with AFP in the previously developed system could not be completely excluded. Because of these reasons, clinical applications of the antibody-lectin EIA detection of fucosylated AFP have not been achieved. The reasons why it is important to develop antibody-lectin EIA of fucosylated AFP are detailed below. i) The enzymatic basis for the reaction and the glycan structures of fucosylated AFP have already been clarified, that is, core-fucosylation by α1,6-fucosyltransferase (FUT8) [23] is the critical reaction (Fig.1) and results in the production of fucosylated AFP [24]. ii) A valid tumor marker should be specific and its detection should make it possible to distinguish clearly between malignant from benign diseases, and fucosylated AFP meets these requirements [12]. iii) It should be possible to quantitatively measure the tumor marker using a simple, straightforward method, such as an antibody-lectin EIA. Fucosylated AFP is currently measured by means of a liquid-phase binding assay (LBA) [25] or by an electrokinetic analyte transport assay (EATA) [26], but these methods require special instrumentation, which constitutes a significant drawback to their use. iv) Sufficient standard antigens for a quantitative analysis should be readily available. This is one of the most important points for clinical applications of the assay method. In our previous study, we developed an easy method for the large-scaled purification of AFP, designated the three-phase partitioned method [27]. v) A specific antibody and lectin should be available, both of which for fucosylated AFP, namely, an anti-AFP antibody and a fucose-specific *Aleuria aurantia* lectin (AAL) are commercially available. vi) Once the method is established, the technique should be generally applicable to a variety of fucosylated glycoproteins by using specific antibodies for each type of glycoprotein. This is a strong point in the development of an antibody-lectin EIA of fucosylated AFP.

In this study, we reinvestigated the development of an antibody-lectin EIA for the quantitative determination of fucosylated AFP, in an attempt to overcome the problems associated with our previous antibody-lectin EIA system. We re-constructed the assay system with a periodate-oxidized anti-AFP IgG, a biotinylated AAL, a peroxidase-conjugated streptoavidin, and a chemiluminescent detection system. Highly fucosylated AFP sample diluted to from 5 to 80 ng/ml in human sera was successfully measured by the developed method, when an enrichment procedure was used in the isolation of AFP.

2. Materials and methods

2.1. Materials

Materials were obtained from the following suppliers: Anti-human AFP rabbit polyclonal antibody from Dako (Glostrup, Denmark); Biotinylated *A. aurantia* lectin (AAL) from Seikagaku Biobusiness (Tokyo, Japan); Horseradish peroxidase (HRP)-conjugated streptoavidin, SuperBlock T20 (PBS) Blocking Buffer, and SuperSignal West Femto Maximum Sensitivity Substrate from PIERCE (Rockford, IL); Bovine serum albumin (BSA) from Nacalai Tesque (Kyoto, Japan); Sodium metaperiodate and borane-dimethylamine complex from Wako Pure Chemicals (Osaka, Japan); and human pooled serum from SIGMA-Aldrich (ST. Louis, MO). Biotinylated *Aspergillus oryzae* lectin (AOL) [28] was generously supplied by Dr. Kengo Matsumura (Gekkeikan Sake Co. Ltd., Kyoto, Japan). Anti-human AFP equine polyclonal antiserum was kindly provided by Dr. Shinzo Nishi (Professor Emeritus, Hokkaido University, Hokkaido, Japan). Anti-human AFP equine polyclonal IgG was purified from the provided antiserum by ammonium sulfate precipitation, DEAE-cellulose (Whatman, Piscataway, NJ) and HiTrap Protein G HP (GE Healthcare, Buchinghamshire, UK) column chromatography and then used as a capture antibody.

Serum samples of patients with hepatocellular carcinoma (HCC), liver cirrhosis, and chronic hepatitis were obtained from Osaka University-Related Hospital (Osaka, Japan). The ethics committee of Osaka University-Related Hospital approved the study protocol, and written informed consent was obtained from each patient.

2.2. Preparation of highly fucosylated AFP

Human gastric cancer FU97 cells are known to be high-level AFP-producing cells [29] and the cells were obtained from Human Science Research Resources Bank (HSRRB, Japan, JCRB1074). The FU97 cells contained substantial endogenous FUT8 activity, and AFP secreted from the cells exhibited high reactivity with AOL which is known to be highly specific to core fucose [28] (data not shown). When we

constructed the FU97 cells stably overexpressing FUT8 cDNA in order to further increase the cellular FUT8 activity and obtain almost perfect core-fucosylation in AFP secreted from the cells, no further increase was found in the reactivity of the secreted AFP with AOL compared to the AFP from corresponding parental cells (data not shown). This suggested the AFP secreted from FU97 cells was already efficiently core-fucosylated by endogenous FUT8 activity. Thus, we decided to use the FU97-cell derived AFP as a highly fucosylated AFP standard in this study. The FU97 cells were cultured in serum-free Dulbecco's modified Eagle's medium (DMEM) and conditioned medium, which contained the secreted fucosylated AFP was collected. The collected serum-free conditioned medium (100 ml) was used as a starting material for each purification process, as follows. All purification steps were carried out at 4 °C. The protein portion of the conditioned medium was concentrated by ammonium sulfate precipitation (75% saturation). The resulting precipitate was re-dissolved in a small volume of 25 mM Tris–HCl buffer (pH 7.5) and then desalted with two tandemly connected HiTrap desalting columns (5 ml × 2, GE Healthcare) that had been equilibrated with the same buffer. The desalted fraction was applied to a HiTrap Q HP column (5 ml × 1, GE Healthcare) that had been equilibrated with the same buffer as the HiTrap desalting column chromatography. The column was washed with 5 column volumes of the buffer and the bound proteins were then eluted with a NaCl gradient from 0 to 0.1 M in 1 column volume, and then from 0.1 to 0.5 M in 19 column volumes. The eluted AFP, the peak of which was detected by SDS-PAGE and by western blotting for AFP, was collected and concentrated with an Amicon Ultra 4 centrifugal filter device (YM-30, Millipore, Billerica, MA). The concentrated fraction was further purified on a Superose 12 HR 10/30 column (GE Healthcare) using 50 mM Tris–HCl buffer (pH 8.0) as the eluting buffer. Fractions containing the eluted AFP were combined and then directly applied to a Mono Q 5/50 GL column that had been equilibrated with the same buffer as that used for the Superose 12 column chromatography. The column was washed with 5 column volumes of the buffer, and the bound proteins were eluted with a NaCl gradient from 0 to 0.1 M in 1 column volume and then from 0.1 to 0.25 M in 19 column volumes. Fractions containing AFP were combined and the buffer in the fraction was replaced by PBS (−), concentrated with an Amicon Ultra 4 centrifugal filter device, and then collected as a standard highly fucosylated AFP (ca. 200 μg, supplementary Fig. S1).

Protein contents were determined using a BCA protein assay kit (PIERCE) using BSA as standard.

2.3. Procedure of antibody-lectin EIA

A microtiter plate (96F MAXISORP White Microwell, NUNC, Roskilde, Denmark) was coated with the purified anti-human AFP equine polyclonal IgG (0.2 mg/ml) dissolved in 50 mM sodium hydrogen carbonate solution at a level of 50 μl/well for 1 h at 37 °C. The plate was washed three times with 0.2 ml/well of PBS (−), and then blocked with 0.1 ml/well of SuperBlock T20 blocking buffer for 1 h at 37 °C followed by washing three times with 0.2 ml/well of PBS (−). After adding 0.1 ml/well of 10 mM sodium metaperiodate ($NaIO_4$) dissolved in 0.1 M sodium phosphate buffer (pH 7.0), the reaction was allowed to proceed for 30 min at room temperature in the dark in order to degrade the *N*-glycans in the capture IgG coated on the plate. After discarding the $NaIO_4$ solution, the plate was treated with 0.1 ml/well of 5 mg/ml BSA in PBS(−) or 0.5 M 2-aminoethanol, both of which contained 0.25 M borane–dimethylamine complex as a reducing reagent, for 90 min at room temperature to block the formed aldehydes in the capture IgG. After washing the plate three times with 0.2 ml/well of PBS (−), 50 μl/well of standard highly fucosylated AFP that had been diluted in PBS(−) containing 0.05% Tween 20 (PBST) or human sera, or the enriched AFP from clinical serum sample was added and the solution was incubated for 3 h at 37 °C. The plate was washed three times with 0.2 ml/well of PBST, and then 50 μl/well of 4 μg/ml of biotinylated AAL diluted in PBS(−) was added. After incubation for 1 h at room temperature, the plate was washed one time with 0.2 ml/well of PBS (−), and 50 μl/well of 50 ng/ml of horseradish peroxidase-conjugated streptoavidin diluted in PBST was added. The reaction was allowed to proceed for 1 h at room temperature and the plate was then washed three times with 0.2 ml/well of PBS (−). After adding 50 μl/well of SuperSignal West Femto detection reagent (PIERCE), chemiluminescent intensity was determined with a microplate reader.

2.4. Enrichment of AFP from human sera

Standard highly fucosylated AFP diluted in human sera or AFP in clinical serum samples was enriched with an immunoaffinity resin as follows. Anti-human AFP IgG-conjugated Sepharose 4 FF (IgG concentration: ca. 0.25 mg/ml resin) was prepared by introducing anti-human AFP equine polyclonal IgG into the NHS-activated Sepharose 4 FF resin (GE Healthcare) according to the manufacturer's instructions. The anti-human AFP-IgG-conjugated Sepharose 4 FF resin (10 μl) was transferred to a plastic tube, and 0.1 ml of standard highly fucosylated AFP diluted in human sera or clinical serum samples was added. After incubation for 1 h at 4 °C with gentle rotation, the reaction mixture was carefully transferred to a filter cup of an Ultrafree-MC centrifugal filter device (HV, 0.45 μm, Millipore), and centrifuged at 7000 *g* for 1 min at 4 °C. The flow-through fraction was discarded and the residual immunoaffinity resin was subjected to three sets of washings with 0.4 ml of PBST and centrifugation at 7000 *g* for 1 min at 4 °C to remove unbound materials. The filter cup, which contained the washed immunoaffinity resin was transferred to a new plastic tube and 90 μl of 0.1 M glycine–HCl buffer (pH 2.5) containing 0.05% Triton X-100 was added to the resin to elute the bound materials. After centrifugation at 7000 *g* for 3 min at 4 °C, the eluate was collected and the solution was rapidly neutralized with 10 μl of 1 M Tris–HCl buffer (pH 9.0). This preparation was used as the enriched AFP fraction.

2.5. Sandwich ELISA of the enriched AFP fraction

The assay plate was prepared by the same procedure as was used for the antibody-lectin EIA, except that a microtiter plate used was a 96F MAXISORP NUNC immunoplate. The enriched AFP preparation (50 μl/well) was added to the prepared assay plate and the sample was incubated for 3 h at 37 °C. After washing the plate three times with 0.2 ml/well of PBST, 50 μl/well of anti-human AFP rabbit polyclonal IgG (0.5 μg/ml) diluted in PBST was added, and the reaction was then allowed to proceed for 1 h at room temperature. After washing the plate three times with 0.2 ml/well of PBST, 50 μl/well of HRP-conjugated anti-rabbit IgG goat antibody (0.1 μg/ml) diluted in PBST was added and the sample was incubated for 1 h at room temperature. The plate was again washed three times with 0.2 ml/well of PBST, and then 50 μl/well of 50 mM citrate buffer (pH 5.0) containing 0.003% H_2O_2 and 0.6 mg/ml of *o*-phenylenediamine was added. The reaction was allowed to proceed for an appropriate period of time up to 15 min, after which the reaction was stopped by the addition of 50 μl/well of 0.5 M H_2SO_4. The color intensity was determined at 492 nm with a microplate reader.

3. Results and discussion

3.1. Construction of antibody-lectin EIA of fucosylated AFP

In this study, using AFP as a model glycoprotein, we attempted to develop a simple and straightforward assay method for the fucosylation of AFP using an anti-AFP antibody and a fucose-specific *A. aurantia* lectin (AAL). The principle of the assay, designated as an antibody-

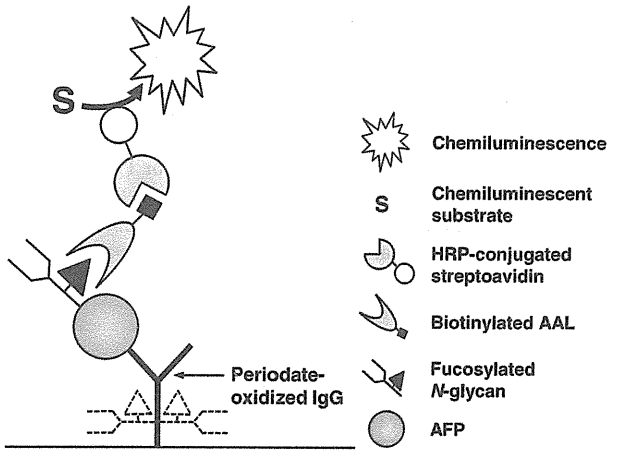

Fig. 2. Schematic representation of the antibody-lectin EIA of fucosylated AFP. AFP was first captured by a periodate-oxidized specific IgG that was coated on a microtiter plate, and the fucose residues in the *N*-glycan in the captured AFP were then successively probed with a biotinylated AAL and horseradish peroxidase (HRP)-conjugated streptoavidin. The amount of the lectin bound to AFP was finally determined by measuring HRP activity using a chemiluminescent detection system.

lectin EIA, is schematically shown in Fig. 2. It is known that *N*-glycans in IgG molecules are core-fucosylated [30]. Thus, if a native IgG were to be used for capturing AFP, AAL would bind to fucose residues in the *N*-glycans of IgG and this would affect the accuracy of the measurement. To prevent this, we selectively destroyed the *N*-glycans in IgG by periodate oxidation (see Materials and methods section), a reagent that cleaves C–C bonds bearing vicinal OH groups in sugars. Subsequent Schiff-base formation and reduction of the formed aldehydes were carried out with a 2-aminoethanol (2-AE) and a borane-dimethylamine complex, respectively. We found that 10 mM periodate was satisfactory for eliminating AAL bound to IgG, and that the reactivity to the antigen of the oxidized IgG was not affected by treatment with such a low concentration of periodate (data not shown). A typical standard curve for highly fucosylated AFP when the constructed antibody-lectin EIA system was used in the absence of human sera is shown in Fig. 3. Using the antibody-lectin EIA, the procedure was sufficiently sensitive to permit the measurement of highly fucosylated AFP in the range of 12.5 to 800 ng/ml with good linearity. Colorimetric detection with an *o*-phenylenediamine or tetramethyl benzidine as HRP substrates was found not to be sufficient for the detection of such a low concentration range of AFP, probably because of its low sensitivity (data not shown). Furthermore,

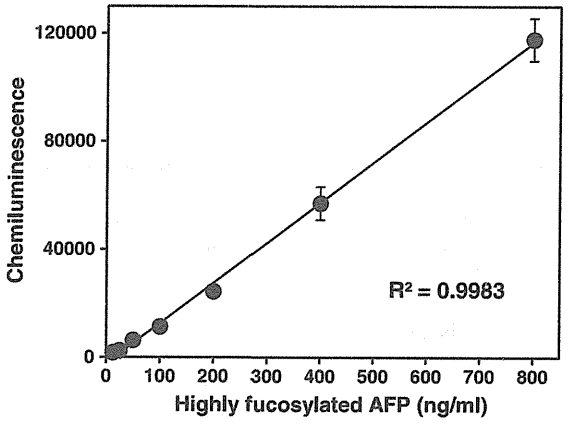

Fig. 3. Antibody-lectin EIA of fucosylated AFP. A typical standard curve of antibody-lectin EIA in the absence of human sera is shown. Highly fucosylated AFP was diluted to 12.5 to 800 ng/ml in PBS(−) containing 0.05% Tween 20. The values are means ± standard deviations for triplicate assays.

fluorescent detection using a fluorescein isothiocyanate (FITC)-labeled AAL was also not successful in determining the amount of the lectin binding to AFP with a high degree of reliability (data not shown). We confirmed that the periodate oxidation of the capture IgG coated on a microtiter plate was very efficient in eliminating background signals derived from the lectin binding to the capture IgG, and in improving the linearity of the standard curve for the highly fucosylated AFP in the antibody-lectin EIA (supplementary Fig. S2).

The reasons why we chose AAL as a probe for fucosylated AFP in the antibody-lectin EIA system were as follows. First, when we tried to construct the system using several fucose-specific lectins including LCA, AOL and AAL, reliable results were obtained in AOL and AAL, but not in LCA. As for LCA, different reaction conditions from those for AOL and AAL may be required, and further experiment optimizing LCA reaction in the system would be needed. Second, the assay result obtained using AAL was far superior to that obtained using AOL in respect to sensitivity and linearity of the standard curve for highly fucosylated AFP (Supplementary Fig. S3). It was found that a high-concentration range of the standard AFP (200–800 ng/ml) was measurable by AOL, but a low-concentration range of AFP (12.5–100 ng/ml) was completely unable to be measured by this lectin.

3.2. Gross inhibition of antibody-lectin EIA by human serum components

After establishing a complete procedure for antibody-lectin EIA of fucosylated AFP in the absence of human sera, it was found that the antibody-lectin EIA in the presence of human sera was intensely inhibited by the increase in background signals (Fig. 4a). The intensity of inhibition was well correlated with the concentration of human sera contained in the assay system, indicating that the inhibition was likely due to components derived from human sera. Over a 2000-fold dilution of human sera was necessary for observing concentration-dependent signals derived from the highly fucosylated AFP in the assay in the presence of human sera. We found that the addition of fucose at a final concentration of 10 mM during the AAL reaction in the assay completely abolished the background signals (Fig. 4b, compare closed and open squares). This finding conclusively indicated that the origin of the background signals was the binding of the lectin to contaminating potentially fucosylated human serum components, probably serum glycoproteins that are highly abundant in sera. We attempted to eliminate the background signals from the assay system by modifying various factors, including the type of blocking reagents used, the use of a Fab capture antibody, the type of medium used to dilute the human sera, the removal of IgG from human sera, the removal of components that could potentially bind to the capture IgG from human sera and so on, but none were satisfactory for eliminating the background signals from the assay system. The background signals were finally eliminated from the assay system by modifying procedure for the periodate oxidation of the capture IgG. We found that the background signals resulting from the interaction of AAL with human serum components in the assay were dramatically attenuated, when BSA was used instead of 2-AE as a blocking reagent for the aldehyde groups formed as the result of the periodate oxidation of the capture IgG (Fig. 4b). Because BSA treatment was completely ineffective once the periodate-oxidized IgG was 2-AE-blocked (data not shown), this preferable effect of BSA on diminishing the background signals in the assay system seemed not to be regarded as a result of a simple blocking of free places on immunoplate by BSA that prevents serum glycoproteins from binding to the plate. Rather, the result indicated that the cause of the increase in the background signals in the assay system was the use of 2-AE as a blocking reagent for the formed aldehydes after periodate oxidation. Human serum likely contains components that bind strongly to the periodate-oxidized and 2-AE-blocked IgG, and these components are potentially fucosylated resulting in a gross inhibition of the antibody-lectin EIA. The BSA bound to the capture

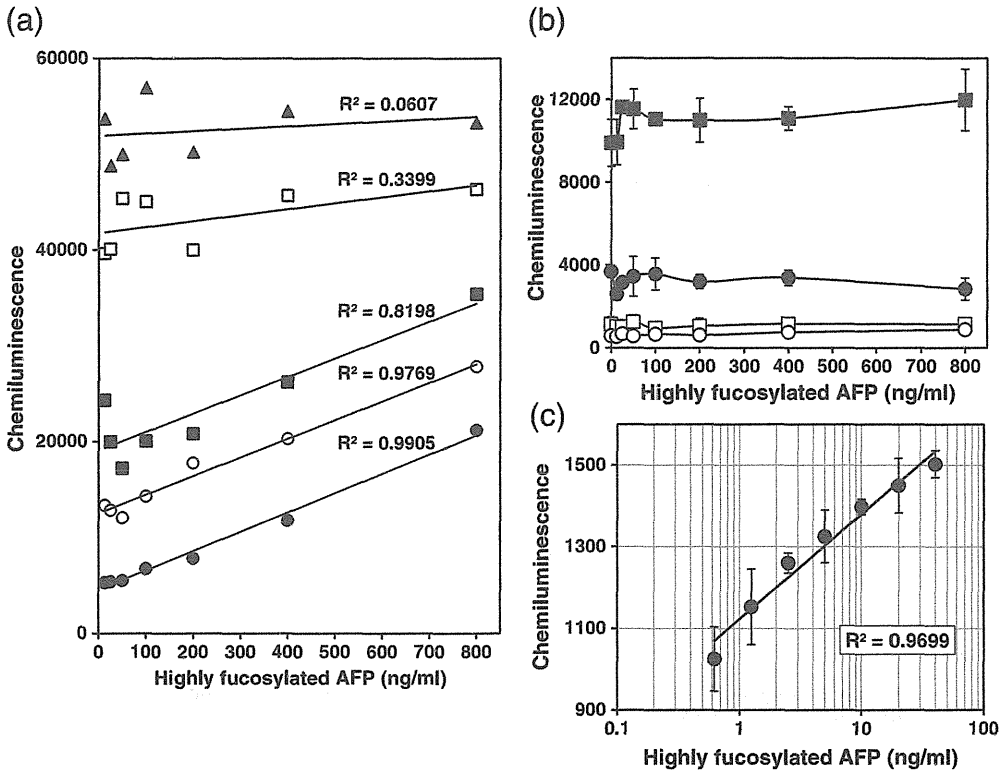

Fig. 4. Effect of using BSA as a blocking reagent for the formed aldehydes in capture IgG after periodate oxidation on antibody-lectin EIA. (a) Results obtained for the assay of highly fucosylated AFP in the presence of human sera are shown. Highly fucosylated AFP was diluted to 12.5 to 800 ng/ml in 10% (closed triangles), 1% (open squares), 0.1% (closed squares), 0.05% (open circles), and 0% (closed circles) human sera which had been diluted with PBS(−) containing 0.05% Tween 20. The values are means for duplicate assays. (b) Results obtained in the assays using 2-aminoethanol (2-AE)- and BSA-blocked capture IgGs. The aldehydes formed in the capture IgG after periodate oxidization were blocked with 2-AE (squares) or BSA (circles). The AAL reaction was performed in the presence (open squares and circles) or absence (closed squares and circles) of the monosaccharide fucose at a concentration of 10 mM. (c) A standard curve obtained in the antibody-lectin EIA using the periodate-oxidized and BSA-blocked capture IgG in the presence of human sera. The data are plotted on a semi-logarithmic scale. Highly fucosylated AFP was diluted to 0.625 to 40 ng/ml in 10% human sera. The values are means ± standard deviations for triplicate assays (b, c).

IgG may efficiently inhibit such potential interactions of serum components with the capture IgG probably because of steric hindrance effects. As a result, all further assays were carried out using periodate-oxidized and BSA-blocked capture IgG. Under these conditions, a relatively good concentration-dependent curve for AAL binding to highly fucosylated AFP diluted in human sera by the antibody-lectin EIA was obtained (Fig. 4c). Because some small background signals remained, even after the use of the BSA-blocked capture IgG (Fig. 4b, see closed and open circles), the possibility that traces of residual contaminated serum components were simultaneously measured with highly fucosylated AFP in the assay system cannot be completely excluded (Fig. 4c).

3.3. Enrichment of AFP was effective in the improvement of antibody-lectin EIA

To overcome the above possibility, we added an enrichment step for AFP from human sera to the antibody-lectin EIA procedure. The developed enrichment procedure for AFP is schematically shown in Fig. 5a. We enriched highly fucosylated AFP diluted in human sera using anti-AFP antibody-conjugated immunoaffinity beads (details are described in the Materials and methods section), and then checked the completeness of the procedure by a sandwich ELISA for AFP. As shown in Fig. 5b, we were able to obtain a clear concentration-dependent curve for the binding of anti-AFP to the enriched highly fucosylated AFP, indicating that the AFP diluted in human sera was captured by and eluted from the immunoaffinity beads in a concentration-dependent manner. As a result, our procedure for the enrichment of AFP from human sera was judged to be sufficient for the separation of AFP from major serum components that cause the increase in the background signals in the assay. We next attempted to measure the enriched highly fucosylated AFP using the antibody-lectin EIA. We succeeded in obtaining a concentration-dependent curve for the binding of AAL to the enriched highly fucosylated AFP in the range of 5 to 80 ng/ml with a correlation coefficient of ca. 0.99 (Fig. 5c).

The developed antibody-lectin EIA system for the determination of fucosylated AFP appears to be superior to the previous system we reported on, especially in sensitivity. In addition, the problem associated with the potential contamination of high-abundant serum glycoproteins in the assay system was easily solved by the enrichment procedure for the AFP from human sera.

3.4. Antibody-lectin EIA of fucosylated AFP in sera from patients with liver diseases

It is known that the normal level of AFP in sera is less than 10 ng/ml, which increases in various benign or more malignant diseases. In particular, the AFP level significantly increases in the cases of hepatocellular carcinoma (HCC) up to 1000 ng/ml or more, but in many cases of early stage of HCC, the level of AFP is 100–400 ng/ml or less. The fucosylated AFP is highly specific to HCC, and the ratio of fucosylated AFP to total AFP increased over 10% can be clinically indicative of HCC. Thus, it could be said that the assay system for fucosylated AFP needs the sensitivity enabling measurement of at least 10–40 ng/ml of fucosylated AFP in sera. Even though validation studies are necessary, we have performed preliminary studies by using clinical samples. We tried to examine the usefulness of the developed antibody-lectin EIA by measuring the fucosylated AFP in the sera from patients with HCC, liver cirrhosis (LC), and chronic hepatitis (CH).

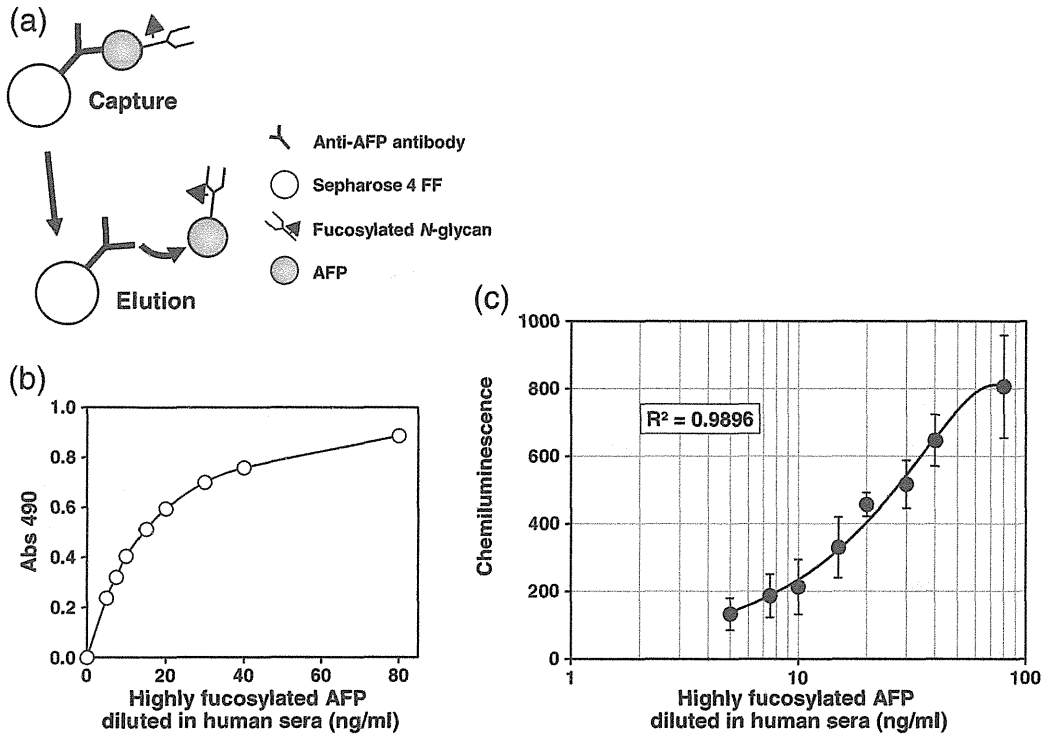

Fig. 5. Effect of the enrichment of AFP from human sera on antibody-lectin EIA. (a) Schematic representation of the enrichment of AFP from human sera. AFP in human sera was captured with anti-human AFP equine polyclonal IgG-conjugated Sepharose 4FF beads. After thorough washing, the captured AFP was eluted by acidifying the buffer and the pH in the eluate was rapidly neutralized. The resulting eluate was used as the enriched AFP preparation. (b) Sandwich ELISA of the enriched AFP sample. Highly fucosylated AFP was diluted to 5 to 80 ng/ml in 10% human sera, enriched as shown in panel a, and then assayed by sandwich ELISA. The values are means for duplicate assays. (c) Antibody-lectin EIA of the enriched AFP fraction. The data are plotted on a semi-logarithmic scale. The values are means ± standard deviations for triplicate assays.

After enrichment of AFP from the serum samples, the fucosylated AFP in the enriched fractions was assayed using the antibody-lectin EIA. As shown in Fig. 6, we could measure the level of fucosylated AFP in clinical samples including HCC, LC, and CH by the developed assay method, but the determined fucosylated AFP levels in all the clinical samples seemed relatively high than we expected. The data were suggestive of the nonspecific reaction caused by the contaminated high-abundant serum glycoproteins especially in the clinical sample assay, even after the enrichment of AFP. A potential solution to the contamination of high-abundant serum glycoproteins would be the large dilution of clinical serum samples, though the assay system is simultaneously required to further increase its detection sensitivity. Validation studies are also needed to evaluate this method for clinical application by using many clinical samples.

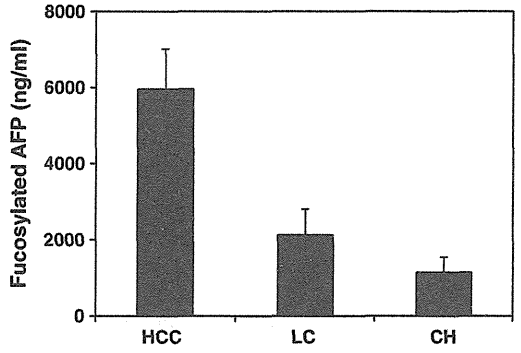

Fig. 6. Antibody-lectin EIA for fucosylated AFP in the sera from patients with liver diseases. Sera from patients with HCC (n = 1), liver cirrhosis (LC, n = 1), and chronic hepatitis (CH, n = 1) were diluted with PBST, and AFP in the diluted serum samples was enriched using anti-AFP antibody-conjugated immunoaffinity beads (Fig. 5a). Highly fucosylated AFP standard was also diluted with PBST and processed by the same procedures as the clinical samples. The level of fucosylated AFP in the enriched fractions was assayed using the antibody-lectin EIA. The values are means ± standard deviations for triplicate assays.

4. Conclusions

Using AFP as a model glycoprotein, we developed a basic technology for a simple assessment of fucosylation of AFP designated antibody-lectin EIA based on a sandwich technique with a periodate-oxidized specific antibody, fucose-specific AAL, and chemiluminescent detection system. The gross background signals derived from human serum components in the assay system were efficiently eliminated by using BSA instead of the conventionally used 2-AE for blocking the formed aldehydes in the capture IgG after periodate oxidation. We were able to quantitatively measure standard highly fucosylated AFP diluted to 5 to 80 ng/ml in human sera by the developed method, when an enrichment procedure for isolating AFP from human sera, using anti-AFP antibody-conjugated immunoaffinity beads, was used. However, because the nonspecific reaction that increases background signals in the assay system seemed too high in the clinical serum samples, large dilution of the sera would be needed for accurate measurement of fucosylated AFP. Large dilution of sera and the AFP level in early stages of HCC are taken into consideration, it would be indispensible to establish a basic technology that greatly increases the detection sensitivity in the antibody-lectin EIA. Although further validation of the assay system will be needed for its clinical application, the basic techniques developed in this study promise to be applicable to measurements of various other fucosylated glycoproteins and would make it possible to easily assess the degree of fucosylation without the need for special instrumentation.

Acknowledgements

We thank Dr. Shinzo Nishi (Professor Emeritus, Hokkaido University) and Dr. Kengo Matsumura (Gekkeikan Sake Co., Ltd.) for providing us with anti-human AFP equine antiserum and biotinylated AOL, respectively. We also thank Dr. Yoshiki Yamaguchi (Systems Glycobiology Research Group, RIKEN ASI), Dr. Nobuto Koyama (Takara Bio Inc.), Megumi Otsuka (Takara Bio Inc.), and Kyoko Kamihagi (Takara Bio Inc.) for their valuable suggestions and discussions. This work was supported by grants from the New Energy and Industrial Technology Development Organization (NEDO) of the Ministry of Economy, Trades and Industry of Japan; the Global COE Program of Osaka University funded by the Ministry of Education, Culture, Sports, Science, and Technology of Japan; the Naito Foundation, and by the grant in relation to "Validation of the treatment protocol using glycosaminoglycans for COPD exacerbation in vitro and Exploring biomarkers associating COPD exacerbation" from the National Institute of Biomedical Innovation in Japan.

Appendix A. Supplementary data

Supplementary data to this article can be found online at doi:10.1016/j.bbagen.2011.12.015.

References

[1] R. Apweiler, H. Hermjakob, N. Sharon, On the frequency of protein glycosylation, as deduced from analysis of the SWISS-PROT database, Biochim. Biophys. Acta 1473 (1999) 4–8.
[2] N. Taniguchi, E. Miyoshi, J. Gu, K. Honke, A. Matsumoto, Decoding sugar functions by identifying target glycoproteins, Curr. Opin. Struct. Biol. 16 (2006) 561–566.
[3] K. Ohtsubo, J.D. Marth, Glycosylation in cellular mechanisms of health and disease, Cell 126 (2006) 855–867.
[4] S. Hakomori, Tumor malignancy defined by aberrant glycosylation and sphingo (glyco) lipid metabolism, Cancer Res. 56 (1996) 5309–5318.
[5] S. Hakomori, Glycosylation defining cancer malignancy: new wine in an old bottle, Proc. Natl. Acad. Sci. U. S. A. 99 (2002) 10231–10233.
[6] R. Kannagi, M. Izawa, T. Koike, K. Miyazaki, N. Kimura, Carbohydrate-mediated cell adhesion in cancer metastasis and angiogenesis, Cancer Sci. 95 (2004) 377–384.
[7] N. Taniguchi, E. Miyoshi, J.H. Ko, Y. Ikeda, Y. Ihara, Implication of *N*-acetylglucosaminyltransferases III and V in cancer: gene regulation and signaling mechanism, Biochim. Biophys. Acta 1455 (1999) 287–300.
[8] T. Morinaga, M. Sakai, T.G. Wegmann, T. Tamaoki, Primary structures of human α-fetoprotein and its mRNA, Proc. Natl. Acad. Sci. U. S. A. 80 (1983) 4604–4608.
[9] K. Taketa, Alpha-fetoprotein: reevaluation in hepatology, Hepatology 12 (1990) 1420–1432.
[10] Y. Aoyagi, Y. Suzuki, K. Igarashi, A. Saitoh, M. Oguro, T. Yokota, S. Mori, M. Nomoto, M. Isemura, H. Asakura, The usefulness of simultaneous determinations of glucosaminylation and fucosylation indices of alpha-fetoprotein in the differential diagnosis of neoplastic diseases of the liver, Cancer 67 (1991) 2390–2394.
[11] K. Taketa, Y. Endo, C. Sekiya, K. Tanikawa, T. Koji, H. Taga, S. Satomura, S. Matsuura, T. Kawai, H. Ilirai, A collaborative study for the evaluation of lectin-reactive a-fetoproteins in early detection of hepatocellular carcinoma, Cancer Res. 53 (1993) 5419–5423.
[12] E. Miyoshi, K. Moriwaki, T. Nakagawa, Biological function of fucosylation in cancer biology, J. Biochem. 143 (2008) 725–729.
[13] B. Tissot, S.J. North, A. Ceroni, P.-C. Pang, M. Panico, F. Rosati, A. Capone, S.M. Haslam, A. Dell, H.R. Morris, Glycoproteomics: past, present and future, FEBS Lett. 583 (2009) 1728–1735.
[14] H. Narimatsu, H. Sawaki, A. Kuno, H. Kaji, H. Ito, Y. Ikehara, A strategy for discovery of cancer glyco-biomarkers in serum using newly developed technologies for glycoproteomics, FEBS J. 277 (2010) 95–105.
[15] S. Chen, T. LaRoche, D. Hamelinck, D. Bergsma, D. Brenner, D. Simeone, R.E. Brand, B.B. Haab, Multiplexed analysis of glycan variation on native proteins captured by antibody microarrays, Nat. Methods 4 (2007) 437–444.
[16] K.L. Abbott, A.V. Nairn, E.M. Hall, M.B. Horton, J.F. McDonald, K.W. Moremen, D.M. Dinulescu, M. Pierce, Focused glycomic analysis of the *N*-linked glycan biosynthetic pathway in ovarian cancer, Proteomics 8 (2008) 3210–3220.
[17] A.D. Taylor, W.S. Hancock, M. Hincapie, N. Taniguchi, S.M. Hanash, Towards an integrated proteomic and glycomic approach to finding cancer biomarkers, Genome Med. 1 (2009) 57.
[18] O. Gornik, G. Lauc, Enzyme linked lectin assay (ELLA) for direct analysis of transferrin sialylation in serum samples, Clin. Biochem. 40 (2007) 718–723.
[19] A. Olewicz-Gawlik, I. Korczowska-Łącka, J.K. Łącki, K. Klama, P. Hrycaj, Fucosylation of serum α1-acid glycoprotein in rheumatoid arthritis patients treated with infliximab, Clin. Rheumatol. 26 (2007) 1679–1684.
[20] M.A. Comunale, M. Wang, J. Hafner, J. Krakover, L. Rodemich, B. Kopenhaver, R.E. Long, O. Junaidi, A.M. Di Bisceglie, T.M. Block, A.S. Mehta, Identification and development of fucosylated glycoproteins as biomarkers of primary hepatocellular carcinoma, J. Proteome Res. 8 (2009) 595–602.
[21] H. Matsumoto, S. Shinzaki, M. Narisada, S. Kawamoto, K. Kuwamoto, K. Moriwaki, F. Kanke, S. Satomura, T. Kumada, E. Miyoshi, Clinical application of a lectin-antibody ELISA to measure fucosylated haptoglobin in sera of patients with pancreatic cancer, Clin. Chem. Lab. Med. 48 (2010) 505–512.
[22] N. Kinoshita, S. Suzuki, Y. Matsuda, N. Taniguchi, α-fetoprotein antibody-lectin enzyme immunoassay to characterize sugar chains for the study of liver diseases, Clin. Chim. Acta 179 (1989) 143–152.
[23] E. Miyoshi, N. Taniguchi, α6-Fucosyltransferase (FUT8), in: N. Taniguchi, K. Honke, M. Fukuda (Eds.), Handbook of Glycosyltransferases and Related Genes, Springer, Tokyo, 2002, pp. 259–263.
[24] T. Nakagawa, E. Miyoshi, T. Yakushijin, N. Hiramatsu, T. Igura, N. Hayashi, N. Taniguchi, A. Kondo, Glycomic analysis of alpha-fetoprotein L3 in hepatoma cell lines and hepatocellular carcinoma patients, J. Proteome Res. 7 (2008) 2222–2233.
[25] H. Katoh, K. Nakamura, T. Tanaka, S. Satomura, S. Matsuura, Automatic and simultaneous analysis of *Lens culinaris* agglutinin-reactive alpha-fetoprotein ratio and total alpha-fetoprotein concentration, Anal. Chem. 70 (1998) 2110–2114.
[26] T. Kawabata, H.G. Wada, M. Watanabe, S. Satomura, "Electrokinetic analyte transport assay" for α-fetoprotein immunoassay integrates mixing, reaction and separation on-chip, Electrophoresis 29 (2008) 1399–1406.
[27] H.F. Deutsch, N. Taniguchi, M.A. Evenson, Isolation and properties of human alpha-fetoprotein from HepG2 cell cultures, Tumor Biol. 21 (2000) 267–277.
[28] K. Matsumura, K. Higashida, H. Ishida, Y. Hata, K. Yamamoto, M. Shigeta, Y. Mizuno-Horikawa, X. Wang, E. Miyoshi, J. Gu, N. Taniguchi, Carbohydrate binding specificity of a fucose-specific lectin from *Aspergillus oryzae*, J. Biol. Chem. 282 (2007) 15700–15708.
[29] M. Matsuda, A. Watanabe, H. Sawada, Y. Yamada, H. Nakano, M. Iwai, Y. Iwai, Establishment of an alpha-fetoprotein-producing cell line derived from gastric cancer, In Vitro Cell. Dev. Biol. Anim. 35 (1999) 555–557.
[30] S. Fujii, T. Nishiura, A. Nishikawa, R. Miura, N. Taniguchi, Structural heterogeneity of sugar chains in immunoglobulin G, J. Biol. Chem. 265 (1990) 6009–6018.